Viscosity, Flow Characteristics and Microstructural Characterization of Industrial Blast Furnace Slags

Dissertation submitted to the

National Institute of Technology Rourkela

in partial fulfillment of the requirements

of the degree of

MASTER OF TECHNOLOGY (RESEARCH)

IN

METALLURGICAL AND MATERIALS ENGINEERING

by

ANINDITA PATI
(Roll Number: 613MM3004)

Under the supervision of

Prof. Santosh Kumar Sahoo

and

Prof. Upendra Kumar Mohanty

July, 2015

DEPARTMENT OF METALLURGICAL AND MATERIALS ENGINEERING

National Institute of Technology Rourkela

Metallurgical and Materials Engineering
National Institute of Technology Rourkela

July, 2015

Certificate of Examination

Roll Number: 613MM3004
Name: ANINDITA PATI
Title of Dissertation: Viscosity, Flow Characteristics and Microstructural Characterization of Industrial Blast Furnace Slags

We the below signed, after checking the dissertation mentioned above and the official record book (s) of the student, hereby state our approval of the dissertation submitted in partial fulfilment of the requirements of the degree of Master of Technology in Metallurgical and Materials Engineering at National Institute of Technology Rourkela. We are satisfied with the volume, quality, correctness, and originality of the work.

Prof. U.K.Mohanty
Co-Supervisor

Prof. Santosh Kumar Sahoo
Supervisor

Prof. P.K.RAY
Member (MSC)

Prof. Mithilesh Kumar
Member (MSC)

Prof. S.C.Mishra
Member (MSC)

Prof. V.D.Hiwarkar
Examiner

Prof. S.C.Mishra
Chairman (MSC)

Metallurgical and Materials Engineering
National Institute of Technology Rourkela

Prof. *Santosh Kumar Sahoo*

July, 2015

Supervisor's Certificate

This is to certify that the work presented in this dissertation entitled "Viscosity, Flow Characteristics and Microstructural Characterization of Industrial Blast Furnace Slags " by "*Anindita Pati*", Roll Number "613MM3004", is a record of original research carried out by him/her under my supervision and guidance in partial fulfilment of the requirements of the degree of *Master of Technology* in *Metallurgical and Materials Engineering*. Neither this dissertation nor any part of it has been submitted for any degree or diploma to any institute or university in India or abroad.

<Supervisor's Signature>

Prof. *Santosh Kumar Sahoo*

Declaration of Originality

I, *Anindita Pati*, Roll Number 613MM3004 hereby declare that this dissertation entitled "Viscosity, Flow Characteristics and Microstructural Characterization of Industrial Blast Furnace Slags " represents my original work carried out as a doctoral/postgraduate/undergraduate student of NIT Rourkela and, to the best of my knowledge, it contains no material previously published or written by another person, nor any material presented for the award of any other degree or diploma of NIT Rourkela or any other institution. Any contribution made to this research by others, with whom I have worked at NIT Rourkela or elsewhere, is explicitly acknowledged in the dissertation. Works of other authors cited in this dissertation have been duly acknowledged under the section "References". I have also submitted my original research records to the scrutiny committee for evaluation of my dissertation.

I am fully aware that in case of any non-compliance detected in future, the Senate of NIT Rourkela may withdraw the degree awarded to me on the basis of the present dissertation.

JULY, 2015

NIT Rourkela

Anindita Pati

ACKNOWNLEDGEMENTS

I thank Dr.S.C.Mishra (HOD, Department of Metallurgical and Materials Engineering, NIT Rourkela) for having provided me the opportunity to do this project work.

I would like to take this opportunity to express my sincere and utmost gratitude to my Supervisor Prof.S.K.Sahoo and Co-Supervisor Prof. U.K. Mohanty, Department Of Metallurgical and Materials Engineering, NIT Rourkela, for their exemplary guidance, valuable suggestions and their incredible patience for supporting me at every step in my endeavour throughout the research work. It would not have been possible for me to carry out this thesis without their assistance and constant encouragement. I never thought this thesis would be completed till the very last minute. I really appreciate their dedication to this thesis. I would like to thank B. Mishra, DalmiaInstitute of Scientific & Industrial Research, Rajgangpur, Odisha for his support in completing my experimental work.

I would be highly obliged to extend our thanks to Mr. Uday Kumar Sahu for his immense support and help rendered while carrying out experiments, without which completion of this thesis would have been at stake.

I would like to express my sincere gratitude to all the faculty members and staff of the department for their constant support, guidance, cooperation and for providing me all sorts of facilities in various ways for completion of this thesis work.

JULY ANINDITAPATI

ROURKELA 613MM3004

CONTENTS

LIST OF FIGURES

LIST OF TABLES

ABSTRACT

Twenty five numbers of Blast furnace slag samples are collected from different operating Indian Blast furnaces. The viscosity, flow characteristics and microstructural characterization of these slag samples are investigated in the present study. Viscosities of these slags are estimated using various models developed by several researchers followed by experimental determination of viscosities of some selected slag samples (using a high temperature viscometer) to predict the best possible model that can be used for the present investigation. The flow behavior of these slag samples is estimated by a heating microscope and is characterized by ST (Softening Temperature), HT (Hemispherical Temperature) and FT (Flow Temperature). Finally, microstructural characterization is performed using XRD (X-Ray Diffraction) and microscopic analysis. On the basis of the viscosity results a comparison is made between the various models bringing about the shortcomings of these mathematical models. It is observed that the estimated viscosities by Iida model are best fitted with the viscosities of slags measured by high temperature viscometer and hence, the viscosity data obtained by Iida model are analysed at length to ascertain the compositional dependence of slag viscosity. It is observed that the industrial blast furnace slag viscosity is greatly influenced by its CaO/SiO_2 ratio, MgO and Al_2O_3 contents. The characteristic temperatures also show a compositional dependence in the slag samples albeit no clear trend is observed when combined effect of all the oxides is considered. XRD and microscopic results show important phases like melilite, akermanite-gehlenite, spinel and merwinite in the slag samples investigated in the present study.

1. Introduction

Slag viscosity is an important parameter to gauge the efficient performance of a Blast furnace (BF). The blast furnace slag viscosity regulates the reaction kinetics of the furnace by controlling the diffusion of ions through the liquid slag to and from the slag metal interface [1]. It also affects the pattern of gas flow inside the furnace and thus controls the heat transfer from the ascending blast furnace gas to the descending blast furnace burden [2]. The basic slag reacts with the burden, reacting and retaining the sulphur in the burden; these phenomena being direct functions of the viscosity of the slag [3]. In addition, the slag viscosity greatly affects the slag metal separation including the tapping of the slag from the furnace. Thus viscosity of slag controls the efficiency of the blast furnace. Ideally the slag in the blast furnace must have an optimum viscosity. A very fluid slag is likely to interfere with the heat balance of a furnace and attack the refractory lining at a greater rate whereas in case of a viscous slags less damage is caused to the refractory lining though the blast furnace process including the slag-metal partitioning and slag tapping are adversely affected [4].On account of the above the blast furnace man is supposed to acquaint himself with the blast furnace slag viscosity to ensure an efficient blast furnace process of iron making. Owing to the associated difficulties and the costly processes of viscosity measurement it is only pertinent to estimate the blast slag viscosity by using mathematical models proposed by several researchers for the purpose. These models are grouped on the basis of their similarities concerning their temperature and compositional dependence [5-6]. On the basis of temperature, these are based on Arrhenius, Weymann-Frenkel or Eyring equations [7-9]. The NPL (National Physical Laboratory) model developed by Mills and Sridhar [10] is based on Arrhenius equation and relates the slag viscosity to the slag structure using a term ‘optical basicity’ of the slag which is function of slag composition. This model has been applied to a number of

metallurgical slags successfully. The model proposed by Ray and Pal is based on Weymann-Frenkel kinetic theory of liquids [10]. There are cases where the models based on the Weymann-Frenkel equation render results in better agreement with experimentally measured viscosity data [11]. The Iida model [11-13] is based on Arrhenius type of equations to establish temperature dependence and also use a parameter B, the basicity index, which is composition dependent.

The study of flow characteristics of blast furnace slag helps to know the softening and melting phenomena in the blast furnace. This can predict the extent and location of the cohesive zone which have direct effect on the blast furnace operation, quality of hot metal and coke consumption [14-25]. The cohesive zone in the blast furnace is bounded by softening iron bearing materials at the top and the bottom is bounded by melting/flowing of the same iron bearing materials. High softening temperature with low flow temperature would form a narrow cohesive zone. This would decrease the distance travelled by the liquid in the furnace and thus decrease the silicon pick up [26-30]. Even the final slag that trickles down from bosh to hearth region would be short slag which means that it will start to flow as soon as it softens. Flow characteristic of the slag is described in terms of four temperatures according to the German Standard 51730: IDT, the initial deformation temperature, symbolizes the surface stickiness. It is important for movement of the material in the solid state; ST, softening temperature which symbolizes the plastic distortion. This temperature indicates the start of plastic deformation; HT, hemispherical temperature which symbolizes the sluggish flow and it plays an important role in the air flow inside the blast furnace and thus controls the heat and mass transfer; FT, flow temperature, controls the liquid mobility i.e. free flow of the slag [26-30]. The final slag should be a ‘short slag’ which is a slag with a small difference between the ST and FT. This short slag acquires liquid mobility and trickles down the furnace as soon as

possible. This exposes fresh sites for the reaction to start again. This helps in enhanced slag-metal reaction rates and this in turn enhances the blast furnace operation and metal quality.

It may be of interest to note that the flow characteristic of a slag may offer some indications about the viscosity of the slag (high/low) but the characteristic temperatures and viscosity of the slag are not inter-related. Viscosity which is a measure of the resistance offered to the flow between two adjacent layers of a fluid which is a function of temperature and obeys the Arrhenius equation. This is not true for the characteristic temperatures which are specific temperatures indicating rheological status of the slag [31-33]. However, both viscosity and flow characteristics are structure dependent. Viscosity values, so also the characteristic temperatures vary as a consequence of polymerization/de-polymerization as well as loosening/tightening of the ionic bonds between the cations and the anions. Hopkins [34] has established this statement with the example of a eutectic with 23.25% CaO, 14.75% Al_2O_3 and 62% SiO_2. This eutectic has a HT (liquidus temperature) of 1170^oC though it is extremely viscous even at 1600^oC with superheat pertaining to more than 400^oC rise of temperature. On this basis viscosity and characteristic temperatures may be considered to be related qualitatively, but it is difficult to predict an interrelation quantitatively.

It has been well established that viscosity and characteristic temperatures of a slag are significantly dependent on the composition of the slag [35-40]. Different phases formed during the operating temperature are responsible for the change in viscosity and characteristic temperatures of the slag [35-40]. Hence, examination of different phases pertaining to composition of the slag may be an important aspect to provide an overall correlation between the composition and viscosity/characteristic-temperatures of the slag.

1.1 Objectives

Based on the understanding explained above, the following objectives are aimed at:

- Estimation of the viscosity of industrial blast furnace slag, collected from various operating blast furnaces in the country, using various viscosity models. Experimental determination of viscosity of some selected slags to predict the best possible model that can be used for the present investigation.
- Measurement of characteristics temperatures (ST, HT and FT) of the slags using a heating microscope.
- Microstructural characterization of the slags using XRD and optical microscopy to examine the difference in viscosity and characteristic temperatures of various slags pertaining to the phases present.

2. Literature Review

2.1 Introduction

In this chapter the structure of blast furnace (BF) slag and the structural dependence of various characteristic properties of the blast furnace slag have been discussed on the basis of available literature. A vivid mention is made of the structural variations caused due to compositional variations and the alternations brought in due to these compositional variations in the characteristics properties of the BF slag namely 'viscosity' and 'flow characteristics' have been discussed at length based on the work of various experimenters.

As agreed by most of the experimenters SiO_2 a covalent oxide, is a major constituent of the blast furnace slag. Al_2O_3, though amphoteric in nature, may also behave like a covalent oxide and the resultant slag with high Al_2O_3 contents may behave like silica melts. Thus in the present chapter structure of pure silica has been discussed followed by structure of binary silicate melts, poly component melts and complex silicate melts. Finally the structure oriented characteristics properties such as viscosity and flow characteristics resulting from compositional variations have been discussed exhaustively on the basis of available literature.

2.2 Structure of Liquid BF Slag

2.2.1 Structure of Pure Molten Silica

The structure of pure liquid silica is very similar to that pure solid silica which assumes a three dimensional continuous network of SiO_2 tetrahedra in which each silicon ion is tetrahedrally coordinated to four oxygen ions while each oxygen ion is linked to two Si^{4+} ions. On melting, this three dimensional structure is retained with the only difference that there may be a change of ions to short range ordering during melting. This absence of long range ordering renders the pure silica melt highly viscous with a high value of activation energy of viscous flow.

In order to make the pure liquid silica with high viscosity (2.9×10^6 poise at 1720^oC) [41], the structure has to be broken into small flow units involving breaking of Si – O bonds (heat of dissociation 104 K cal $mole^{-1}$) [42].The flow units being that which require the least energy of transfer from the initial unbroken structure to the final transition state. It is suggested [43] that this flow unit is a SiO_2 molecule requiring the least energy of transfer from the initial to the transition state.

Owing to the high viscosity and high activation energy of viscous flow in pure molten silica at any instant of time only a small fraction of the melt may exist in the form of SiO_2 molecules. These SiO_2 molecules are formed from the three dimensionally bonded lattices and take part in the process of flow.

2.2.2 Structure of Binary Silicate Melts

The Blast furnace slag is actually a complex oxide melt consisting of various basic oxide constituents associated with the molten silica. Thus a binary silicate melt, poly component silicate melt and/or complex silicate melt may constitute the resultant slag. An attempt is made here to discuss these melts serially on the basis of the influence of these additive oxides simply/collectively on the pure molten silicate structure and its influence on the properties of the slag.

On adding a basic metal oxide to the molten silica, the added oxygen ion enters the silicate network and separates the corners of the two tetrahedra. On the other hand, the added cation remains adjacent to the negative charge, as shown below.

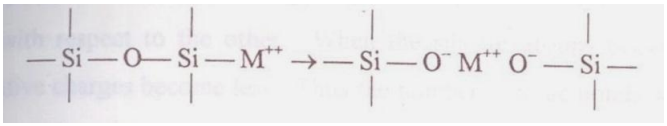

---------- [Eq. 1]

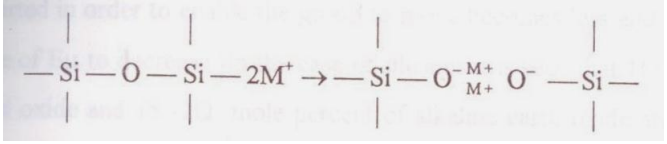

---------- [Eq. 2]

Thus the net result of addition of the basic oxide to the molten silicate network is that it breaks the oxygen bridges between the groups. The driving force for this breakdown is the attraction between the cation (M^{++} or $2M^{+}$ as the case may be) and the unshared oxygen which is also known as the non-bridging oxygen (NBO). Divalent metal cations tend to link the network by bridging two oxygens, while monovalent ones do not [44]. Progressive breaking of the oxygen bonds with the formation of O^{-} (non-bridging oxygen) followed by the formation of O^{2-} (free oxygen) results when more and more basic oxides are added gradually to the molten silica network. The breakdown of the silicate network results in the formation of smaller and smaller silicate groups known as anionic groups or flow units. The additions of more and more network breaking cations do not alter the nature of the anionic groups but encourage the formation of more depolymerized units. The cations, which one randomly distributed in the lattice, result in the following:

i. Weak points are introduced in the SiO_2 network by the breakdown of Si – O bond and
ii. Si – O bonds near the metal ion are weakened due to the polarization effect of the cations. These effects bring in a general loosening effect into the lattice resulting in a general collapse of the lattice as shown in Fig.2.1.

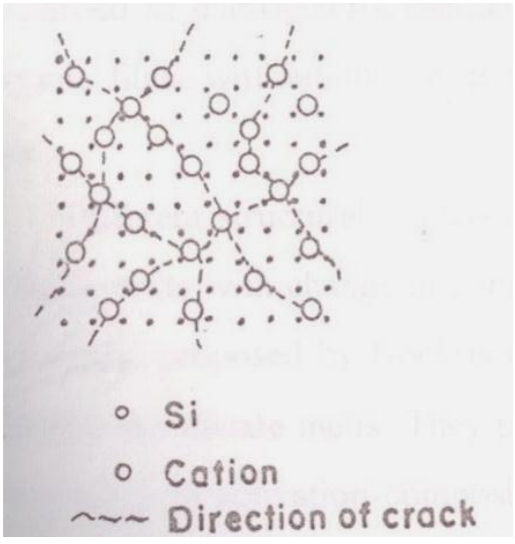

Fig.2.1. Mechanism of collapse of silicate structure [26].

It must be noted, however, that since smaller flow units need higher oxygen for their formation, progressive additions of metal oxides is less and less effective in reducing the flow unit size. This is why increased additions of metal oxide result in decrease of the viscosity only at a decreasing rate, the viscosity of the melt being proportional to the size of the flow unit. Due to the fact that at equimolar compositions there are twice as many monovalent cations as divalent ones and that the divalent cations tend to maintain a continuous bonding of the lattice by bridging oxygen atoms, the effect of monovalent and divalent oxides on the activation energy (E_μ) of viscous flow and viscosity of the melt are different. This explains why addition of Gr. II metal oxides bring in the decrease of E_μ (activation energy) at slower rate, the cationic species having no effect of E_μ till about 55 mole percent whereas Gr. I metal oxide decrease the E_μ value when added in excess of 35 mole percent only [45]. Gr. I metal oxides include Lithium oxide, Rubidium oxide, Sodium oxide, Potassium oxide etc. These are called as alkaline oxides. Gr. II metal oxides include Beryllium oxide, Magnesium oxide, Calcium oxide, Strontium oxide etc. These oxides are known as alkaline earth oxides.

Another consideration is the size of the added metal oxide cation, smaller the cation size less efficient it is in reducing the viscosity, bringing down the E_μ. Here due to steric effect, columbic interactions between metal cations and singly bonded oxygen will be stronger for smaller cations. Thus MgO is not as effective in bringing down the viscosity of the melt as CaO or SrO. Z/r^2 is a parameter (where Z is the valency of the cation and 'r' is the radii) based on which the ability of the cation to form more depolymerized or more polymerized anionic units is decided. This is in the order $Mg^{++} > Ca^{2+} > Sr^{2+} > P_6^{2+} > Ba^{2+} > Li^+ > Na^+ > K^+$. Also, it must be noted that addition of Na_2O, an alkali metal oxide, is more effective in bringing down the viscosity as compared to CaO, an alkali earth cation, since the addition of alkali metal cation (Na_2O) does not enhance the effectiveness of bridging tendency ($O^- - O^-$ interactions).

Different structural models have been proposed to explain the change in properties of silicate melts with change in composition. As explained below, the chain formation concept and the discrete anion model, proposed by Bockris and co-workers [43, 44, and 46] is the most successful model for the silicate melts. According to these researchers, the structure consists of discrete silicate ions. At O: Si ratio 4:1, these discrete ions are SiO_4^{4-} ions. When O: Si ratio is reduced to 7:2 (at 60 mole %CaO i.e. at the stoichiometric composition of $3CaO: 2SiO_2$), the discrete ions can be represented by the reaction given below:

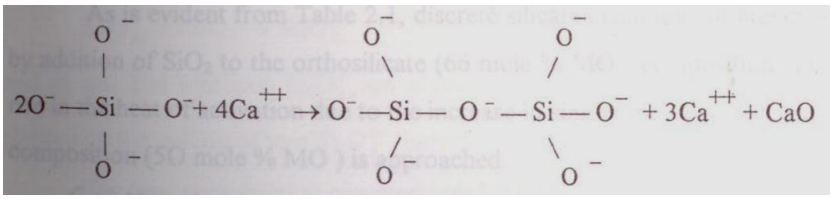

---------- [Eq.3]

On further addition of SiO_2, i.e. when CaO is less, more polymerization is caused and the discrete silicate chain ions now become the flow units. On the basis of this polymerization, on addition of SiO_2 it is proposed that at 52 mole % CaO the long chain silicate ions are replaced by smaller rings as the flow units. The stoichiometric reactions suggested for the formation of these flow units are:

$$2Si_{12}O_{37}^{26-} + SiO_2 \rightarrow 8Si_3O_9^{6-} + SiO_4^{4-} \text{---------- [Eq. 4]}$$

$$Si_{12}O_{37}^{26-} + SiO_4^{4-} \rightarrow Si_7O_{22}^{16-} + Si_6O_{19}^{14-} \text{---------- [Eq. 5]}$$

It must, however, be clearly understood that the concept of these discrete chain ions for a given stoichiometric composition depends only on electro-neutrality considerations. Though, the discrete ion theory explains most of the experimental findings for simple binary silicate melts, it completely ignores the presence of free oxygen (O^{2-}) which must increase with the presence of more and more metal oxides, contributing the metal cations. Thus, the model is not perfect and on this ground Toop and Semis [47-49] suggested an alternative theoretical model based on polymerization/de-polymerization of silicate melts. Toop and Semis agreed to the suggestions of Fincham and Richardson [50] that the reactions deciding

polymerization/de-polymerization in a melt should be of a general type, and should be the same for all compositions. The general equilibrium equation proposed by them is:

$$2O^- \rightarrow O^0 + O^{2-}$$ ---------- [Eq. 6]

for which the equilibrium constant 'K' is given as

$$K = (O^0)\,(O^{2-})/(O^-)^2$$ ---------- [Eq. 7]

Where (O^-), (O^o) and (O^{2-}) represent the numbers of mole of singly bonded, doubly bonded and free oxygen respectively, per mole of the silicate slag. 'K' is a function of temperature and composition of the melt, especially the cation species present in the melt. The significance of this reaction can be seen in the following reactions:

$$2SiO_4^{4-} \rightarrow Si_2O_7^{6-} + O^{2-}$$ ---------- [Eq. 8]

$$8O^- \rightarrow O^0 + 6O + O^{2-}$$ ---------- [Eq. 9]

$$2O^- \rightarrow O^0 + O^{2-}$$ ---------- [Eq. 10]

$$SiO_4^{4-} + Si_2O_7^{6-} \rightarrow Si_3O_{10}^{8-} + O^{2-}$$ ---------- [Eq. 11]

$$10O^- + O^0 \rightarrow 8O^- + 2O^0 + O^{2-}$$ ---------- [Eq. 12]

$$2O^- \rightarrow O^0 + O^{2-}$$ ---------- [Eq. 13]

These reactions show that when two silicate anions polymerize, the resultant reaction reduces to reaction.

$$2O^- \rightarrow O^0 + O^{2-}$$ ---------- [Eq. 14]

However, there are no simple methods of finding out 'K' and one has to guess the value of 'K' and see if the calculated (O^{2-}) values satisfy the observed activity values for the metal oxide over the entire composition range. For this one can use Temkin's model [51] which proposes that $a_{mo} = N_O^{2-}$, where a_{mo} is the activity values for the metal oxide over the entire composition range and N_O^{2-} is the number of moles of oxygen.

Masson [52-55] proposed a model applicable to melts more basic than metasilicate composition (O/Si>3). This model can be used to determine the distribution and molecular

weights of discrete silicate ions present in the melt. The authors suggest that in binary silicate melts (MO – SiO_2) with a sufficiently high ratio of metal oxide and SiO_2, the process of de-polymerization is assumed to complete and silicate is present entirely as discrete SiO_4^{4-} ions. When SiO_2 content is increased, a series of polymerization reactions is assumed to occur resulting in the formation of various chains accompanied by the elimination of one oxygen ion at each step. The equations can be given as:

$$SiO_4^{4-} + SiO_4^{4-} \rightarrow Si_2O_7^{6-} + O^{2-}, (K_1)\text{---------- [Eq. 15]}$$

$$SiO_4^{4-} + Si_2O_7^{6-} \rightarrow Si_3O_{10}^{8-} + O^{2-}, (K_2)\text{---------- [Eq. 16]}$$

$$SiO_4^{4-} + Si_3O_{10}^{8-} + O^{2-}, (K_3)\text{ ---------- [Eq. 17]}$$

Here K_1, K_2, K_3 are equilibrium constants for each step of polymerization and

$$K_1=K_2=K_3\text{---------- [Eq. 18]}$$

In the above equations if the value of 'K' is known, N_{SiO4}^{4-} can be expressed as a function of No^{2-}. Thus when K = 0, only SiO_4^{4-} ions are present in the melt. With increase of 'K', N_{SiO4}^{4-} decreases, the maximum distribution being shifted to higher values of N_O^{2-}. It is true that for any composition, SiO_4^{4-} constitutes the most abundant species followed by $Si_2O_7^{6-}$, $Si_3O_{10}^{8-}$ and so on. This holds good for all compositions and all values of K. Masson [52] also suggests that the nature of cation present determines the tendency of polymerization in silicate melts. The average chain length is thus determined by the extent of cation – silicate ion and cation – oxygen ion attractions. While cations with higher ion, oxygen attraction (Ca^{++}) suppress the process of polymerization cations with weaker ion – oxygen attraction (Mn^{2+}, Fe^{2+}) support the process of polymerization. Masson's treatment, however, have the following limitations. It is applicable only to binary systems. 'K' and No^{2-} must be accurately known for which it imperative that experimentally determined activity data of metal oxides in the melts be known. The model applies to only highly basic silicate melts where the silicate ions are mostly SiO_4^{4-}. Gaskel [56] studies the approaches made use of by several researchers

[49, 54] in their models and listed the various approaches of these experimenters in un-structuring their models. These one summarized below:

i. Generalized polymerization – de-polymerization equilibria involving the three forms of oxygen in the silicate melt and consideration of equilibria among the discrete chain silicate ions and free oxygen ions.
ii. Use of principle of polymer theory to estimate the most probable distribution of branching chain silicate ions.
iii. Adoption of statistical mechanics for calculation of mixing properties.
iv. Monte Carlo minimization of free energy and
v. Adoption of statistical methods to estimate the distribution of silicon oxygen in quasi – lattice [57].

Lacy [58] proposed an altogether different model. He proposed that over a range of O/Si ratio the discrete ions formed a relatively small fraction of the total volume and that the rest of the volume consists of network structure containing branched and cross–linked chains. He suggested, for an example, that when the melt has an O/Si = 2.3, only 3.7 % of the total number of tetrahedra are associated with discrete anionic groups whereas in meta silicate melts (O/Si=3), the corresponding figure is 62.5 %. Mysen [59] suggests the following concerning the structure of binary silicate melts. According to him the structure of the silicate melts are affected by:

i. The nature of the network breaking cation (Ca^{++}, Mg^{++}).
ii. The fitting of certain cations into the silicate network (e.g. Al^{3+}, Ti^{++}) and
iii. The degree of polymerization in the silicate melts.

Investigations are conducted by means of a high temperature X-ray diffraction technique. The following are recorded: Molten silicate consists of SiO_4 tetrahedra units

mainly (up to 57 mole% alkaline earth metal oxides); the structure of molten silicates is insensitive to temperature within the range of temperature investigated.

2.2.3 Structure of Poly-component Silicate Melts

It is inferred by Mackenzie [60] that the mechanism of flow of a binary melt is identical to that of a poly-component silicate melt which may contain more than one group of cations of the same groups. However, the total molar concentration of metal oxides in both the cases (binary and poly-component) must be the same. Thus, ternary silicate melt with cations of different groups are considered as an ideal mixture of two binary melts and the activation energy of viscous flow of the ternary melt can be determined as follows:

$$E_\mu = n_A(E_A)_X + n_B(E_B)_X \text{---------- [Eq. 19]}$$

Where n_A and n_B are mole fractions of the two constituent metal oxides and E_A and E_B, E_μ values of the two groups of the metal oxides. On the above basis when E_μ is computed for even a silicate melt with four different cations, the result is seen to be satisfactory. Thus, it can be concluded with fair accuracy that the discrete ion theory that applies to the binary melts is also applicable to poly-component melts and that the mechanism of flow in both the cases is identical provided in both the cases the molar concentration of SiO_2 is the same. On the basis of the above findings Mackenzie [60] proposed that

$$\log \mu = (\alpha + \beta c) + (\gamma + \delta c)/2.303RT \text{---------- [Eq. 20]}$$

Where α, β, γ and δ are constants and 'c' is the total molar concentration of metal oxides. Mackenzie [60] further proposed the following equation for calculating the viscosity of poly-component melts.

$$\mu = n_A(\mu_A)_c + n_B(\mu_B)_c \text{---------- [Eq. 21]}$$

The calculated and the measured values of viscosities of the poly-component melts are found to be in good agreement. Thus, he inferred that mechanism of flow in binary and

poly-component melts are identical provided the total molar concentration of silica in both binary and poly-component melts are the same.

2.2.4 Structure of Complex Melts

The actual blast furnace slag i.e. the slag emanating from an industrial blast furnace is complex in nature, in the sense that these slags contain Al_2O_3, CaO, MgO, FeO etc. in addition to different amounts of silica.

An attempt is made here to analyze the effect of these oxides individually and collectively in the presence of each other, on the liquid silica thus influencing the various properties of the resulting blast furnace slag.

2.3 Role of Al_2O_3, MgO, CaO and FeO on the structure and structure dependent properties of silicate melts

Polarisability of oxygen ions decides the co-ordination of Al^{3+} ions and thus Al_2O_3 may be present in the form AlO_4 or AlO_6 in the silicate melts [61]. Presence of K^+, Na^+ ions with weaker potential fields permit the formation of AlO_4, allowing O^- ions to polarize to a considerable extent. However, ions with a strong potential field, like Li do not allow the O^- ions to polarize. As a consequence the O^- ions are tightened to such an extent that Al^{3+} ions need more than four O^- ions for its screening and the formation of AlO_6 is favored. When the cation to anion ratio is adjusted so that electro-neutrality is maintained, Al adopts a four-fold co-ordination with oxygen substitutes for silicon ion in the linked tetrahedral structure [62, 63]. In this case the melt contains SiO_4^{4-} and AlO_4^{5-} ions and there are sufficient basic oxides present in the melt with the ratio of Al_2O_3/CaO value being less than unity. However, when Al_2O_3/CaO is more than one i.e. when sufficient basic oxides are not present in the silicate melt, Al adopts a six fold co-ordination with oxygen and enters the interstices in the silicate structure [64]. As a result of the above the complex alumino-silicate anions are disintegrated.

In this way Al_2O_3 in silicate melts can act both as a network former or a network modifier. Thus, when sufficient basic oxides are not present, i.e. when Al adopts a four-fold coordination with oxygen, Al acts as a network former favoring the formation of polymeric ions. It is suggested [63] that these polymeric ions may be of the form:

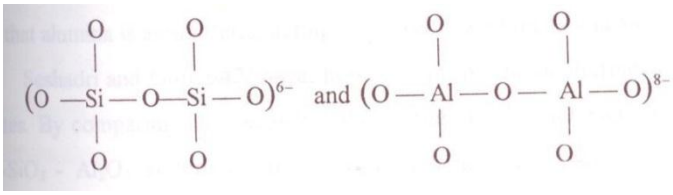

---------- [Eq. 22]

When the alumina and/or silica ions are increased in the melt, more of these polymeric ions are formed in the melt and when lime and/or magnesia contents in the melt are increased, the extent of presence of these polymeric ions in the melt is decreased meaning at least disintegrations of anions in the melt thus enabling Al_2O_3 to act as a network modifier. Three distinct situations emerge [62]:

1. CaO/Al_2O_3 ratio greater the one: Al_2O_3 gradually thickens the melt.
2. CaO/Al_2O_3 ratio equal to one: All Al^{3+} ions present, adopt a tetrahedral arrangement.
3. CaO/Al_2O_3 is less than one: Only a part of Al^{3+} ion adopts a four-fold co-ordination with oxygen, the rest adopting a six-fold co-ordination with oxygen form AlO_6 and causing disintegration of the alumino–silicate anions.

It may thus be inferred that in neutral and basic slags, where Al_2O_3/CaO is less than or equal to unity, Al_2O_3 and CaO behave similarly. Under such conditions both Al and Si occurring similar sites in the lattice and the total network forming ions will be Al + Si. An alternative model has also been proposed to explain the structure of alumino–silicate melts [65]. In this new model, Al with a valency of three is considered to be bonded to three oxygens only as shown in Fig. 2.2.

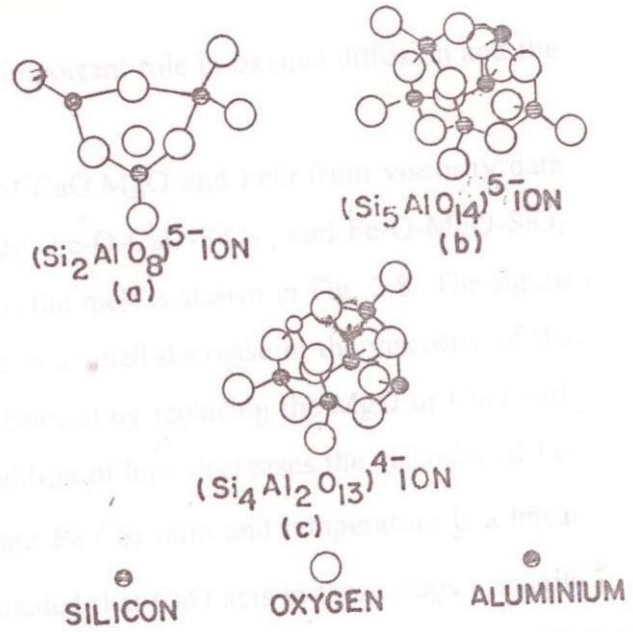

Fig.2.2. Discrete anions in liquid Aluminum Silicates [26].

Basing on this consideration it is suggested [66] that in silicate melts behaving Al_2O_3, Al^{3+} -O^- type of interactions are also present in addition to Ca^{++}-O^- and O^- - O^- interactions, resulting in an increase in the activation energy of viscous flow. Thus, viscosity of the silicate melt will also depend on these interactions and the flow unit size cannot be the only consideration for predicting the viscosity values of the alumino–silicate melts. At a given temperature and for a given viscosity the silica equivalence of alumina (N_a) is given by the difference between the silica concentrations of binary and ternary melts [67] i.e., $N_a = N_{SiO2}$ (binary) – N_{SiO2} (ternary). Silica equivalence of alumina, as related to molar Al_2O_3/CaO ratio and molar alumina concentration, in CaO – SiO_2 – Al_2O_3 melts has been plotted in Fig. 2.3.

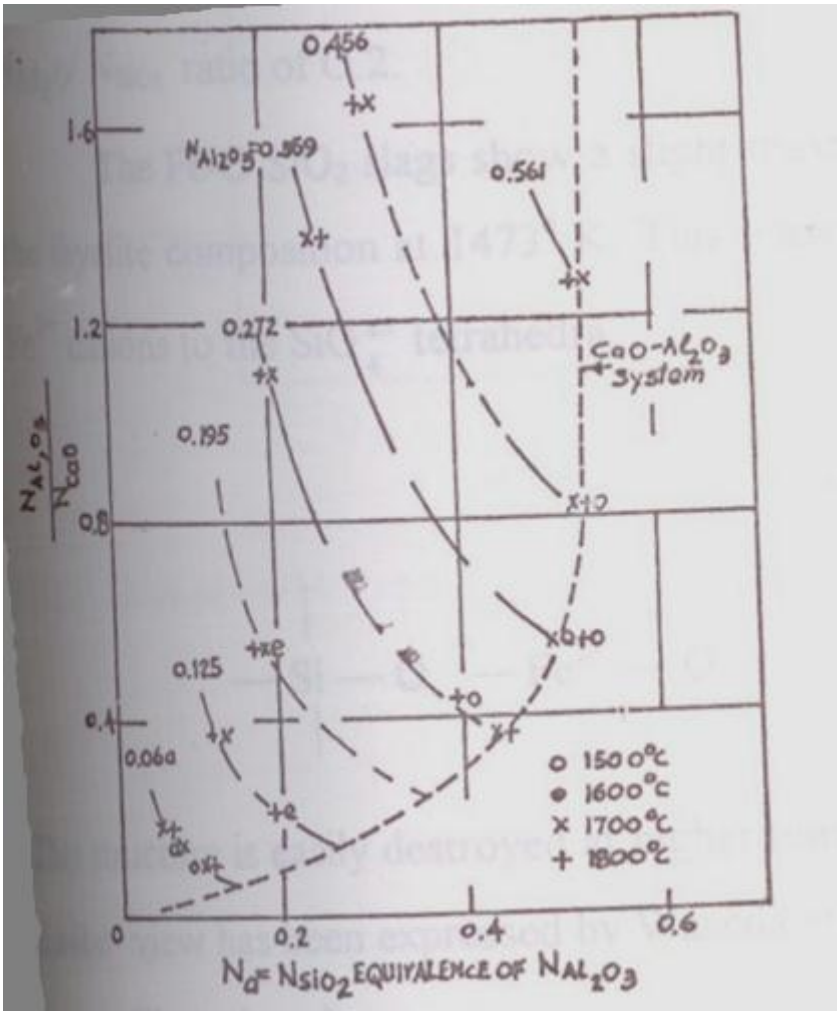

Fig 2.3. Silica equivalence of alumina, N_a, related to molar Al_2O_3/CaO ratio and molar alumina concentration in CaO-SiO_2-Al_2O_3 melts [26].

The Fig. 2.3 reveals the relationship between N_a, Al_2O_3/CaO ratio and Al_2O_3 concentrations within the range of compositions studied by Kozakevitch [62]. Dotted lines in the figure represent the curves corresponding to binary CaO-Al_2O_3 system. A modified version of the diagram supposed to be more useful is presented in Fig. 2.4 given below.

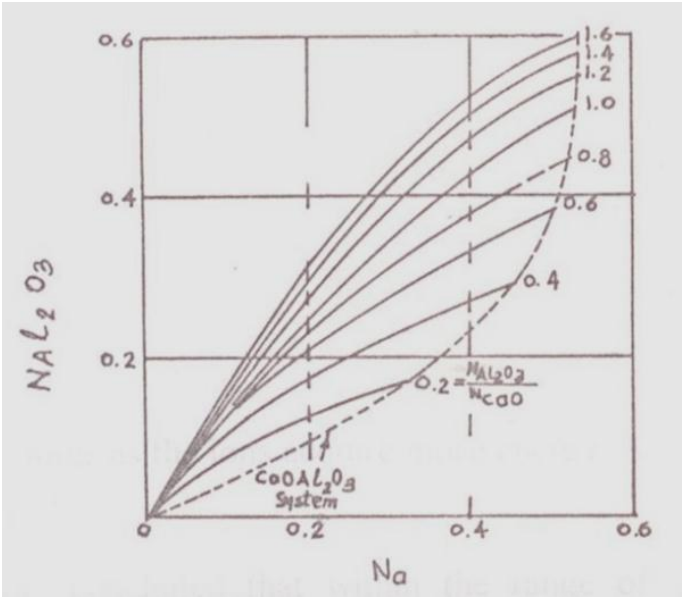

Fig. 2.4. Silica equivalence of alumina related to molar alumina concentrations and molar Al_2O_3/CaO ratio in CaO-SiO_2-Al_2O_3 melts [26].

Here mole function of Al_2O_3 has been plotted against N_a pertaining to different Al_2O_3/CaO ratios. Based on analysis of the experimental data it is proposed [67-69] that while basic oxides like CaO and MgO primarily act as diluents and less a slag modifiers, FeO could be a stronger modifier compared to the two. It is also proposed [59, 70] that ferric ion (Fe^{3+}) acts as network former or network breaker adopting either a four-fold or a six-fold co-ordination. The experimenters suggest that for slags with 10% Fe_2O_3, a four-fold co-ordination is favored with Fe^{3+}/ (Fe^{3+} + Fe^{2+}) ratio is greater than 0.5 and six-fold co-ordination when the same ratio is less than 0.3. It must be appreciated, however, that in most of the practical slags Fe^{3+} ion adopts a four-fold co-ordination and thus, works as network modifier. Bills [71] reports that when less than 15% FeO content, then more FeO is added to the silicon melt the addition is equivalent to the addition of MgO on a molar basis. However, at higher FeO contents the relationship is not valid. Drill reports that the reason of the above loss is the difference in electrostatic binding forces which find Fe^{2+} and Mg^{2+} contains to the silicate ion. Bills [71] further observes that when FeO is gradually added to the silicate melt up to 15 wt%, the resultant viscosity is decreased for the CaO–MgO–Al_2O_3–SiO_2 quaternary

slags and that the addition of higher amounts of FeO is more effective in decreasing the viscosity at higher temperature only. The addition of iron oxide to silicate melts results in the breaking up of silicate anions, providing free oxygen ions as indicated below.

$$FeO = Fe^{2+} + O^{2-}$$ ---------- [Eq. 23]

$$Fe_2O_3 = 2FeO^{2+} + O^{2-}$$ ---------- [Eq. 24]

Effect of FeO in decreasing the slag viscosity is more prominent in acid slags as compared to that in basic slags, as FeO in acid slags can break up silicate anions more effectively in comparison to basic slags. This is because in basic slags the trivalent iron exists mostly in the form of ferrite anions which cannot contribute free oxygen ions for breaking the silicon anions. Thus, it can be concluded that viscosity for acid slags strongly depend on temperature at low iron oxide content and at higher values the same dependence is weak. However, in the case of basic slags the dependence of viscosity on temperature is weak at all values of FeO content.

It is reported [72] that the additions of minor constituents like Sulphur, MnO, FeO, K_2O etc decrease the viscosity of the $CaO–MgO–SiO_2–5\%Al_2O_3$ system. Mysen [59] suggests that cations such as Al^{3+}, Fe^{3+}, B^{3+}, Ti^{4+} and P^{5+} can term tetrahedral (such as AlO_4^{5-}) which fit into the 3-D silicate units and enhance the overall degree of polymerization of the melt. Morinaga [70] reports that Ti can adopt a four-fold or a six-fold co-ordination and these can be a network former or network modifier. 1 to 7 mass percent additions of TiO_2, Ti acts as a network former forming titanates and alumino-titanates.

2.3.1 Measure of the Degree of Polymerization

The property of silicate melts is a function of its structure [73], more specifically the degree of polymerization in the melt. It is in this content it is most pertinent that the measure of the degree of polymerization is discussed of this stage. As suggested by Mills [74]; the

factor NBO/T is the best measure of the degree of polymerization. Here 'NBO' is the number of non–bridging oxygen and 'T' is the tetrahedral coordinated atom. The ratio NBO/T is calculated as follows:

$$Y_{NB} = \sum \begin{matrix} 2[x(CaO) + x(MgO) + x(FeO) + x(MnO) + x(Na_2O) + x(K_2O) + \\ 6(1-f)x(Fe_2O_3) - 2x(Al_2O_3) - 2f(Fe_2O_3)] \end{matrix}$$ ----- [Eq. 25]

$$X_T = \sum x(SiO_2) + 2x(Al_2O_3) + 2fx(Fe_2O_3) + x(TiO_2) + 2x(P_2O_5)$$ ----------[Eq. 26]

$$\frac{NBO}{T} = Y_{NB}/X_T$$ ----------[Eq. 27]

Optical basicity of the melt 'Λ' provides an alternate method for the measure of the degree of polymerization; 'Λ' represents the power of an oxide to donate a negative charge. In general 'Λ' provides a measure of the concentration of O^o, O^- and O^{2-} ions in the melt [75]. 'Λ' can calculated using the following equations.

$$\Lambda = (\sum x_1 n_1 \Lambda_1 + x_2 n_2 \Lambda_2 + x_3 n_3 \Lambda_3 + \cdots) / \sum (x_1 n_1 + x_2 n_2 + x_3 n_3)$$ ---------- [Eq. 28]

Mills [74] provides a method for calculation of Λ_{cor} ($\Lambda_{corrected}$). The optical basicity in value of various oxides is presented below in the Table 2.1. Λ_s is the optical basicity of individual oxides. It is used in the calculation of Λ in Ray and Pal Method and NPL method.

Table 2.1. Values of Λ_s used in the calculation of Λ [74].

oxide	K_2O	Na_2O	BaO	SrO	LiO_2	CaO	MgO	Al_2O_3	TiO_2	SiO_2	B_2O_3	P_2O_5	FeO	Fe_2O_3	MnO	CaF_2
Λ_s	1.4	1.15	1.15	1.10	1.0	1.0	0.78	0.60	0.61	0.48	0.43	0.40	1.0	0.75	1.0	0.43

The ratio Z/r^2 is also used [59] to measure the effect of different cations on the structure and hence the structure dependent properties of various silicates melt. Here Z and r are respectively the valence and the size (radius) of the cation. Z/r^2 is inversely proportional to the optical basicity of different oxides as shown in Fig.2.5.

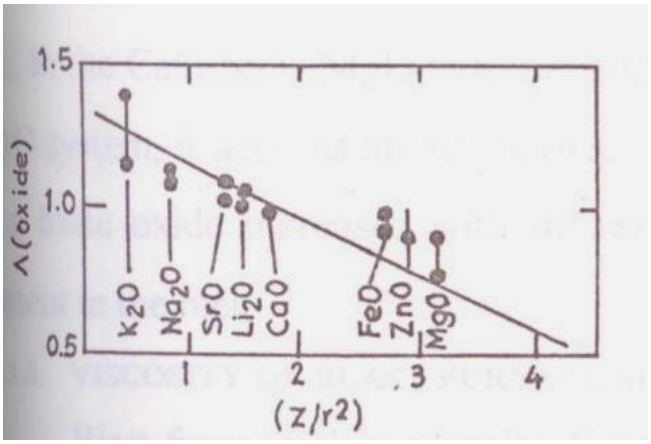

Fig.2.5. The parameters (Z/r^2) as a function of the optical basicity Λ [26].

2.4 Properties of Liquid Slags

2.4.1 Viscosity

The ionic structure of various metallurgical melts affects various properties like viscosity density, ionic conductivity, etc. of the melt. Alternately, a measure of these properties immensely helps the prediction of ionic structures of these melts. The interaction amongst the various anions present in the metallurgical melt decides the viscosity of the melt. It must, however, be noted that these interactions are highly dependent on the composition i.e. the presence of various cations and anions in the melt and the thermal conditions of the melt.

It is of great interest to the operator that the viscosity of metallurgical slags, which is a function of the composition of the slag and the size and type of the structural units present in it, has an important influence on furnace operations. Viscosity is the prime requisite to study the reaction rates in the furnace as it greatly influence the diffusion of ions through the liquid slag to and from the metal / slag interface. A high viscosity of the slag increases the slag – metal exchange rate by increasing the residence time of the dissuading metal droplet in the slag whereas a slag with low viscosity assists slag – metal separation. Also a slag with low viscosity allows a higher rate of heat transfer between the slag and the metal phases by

convection. A slag with high viscosity does not affect the furnace refractory lining to any great extent by its corrosive attacks. Due to these important effects of the slag viscosity as influenced by its composition, structure and temperature, it is important that the viscosity of the slag generated in a metallurgical furnace must be well understood along with the effect of the various factors that affect it.

Plots between logμ (μ-viscosity) and (I/T) (T-Temperature) are reasonably linear, establishing the experimental relationship between viscosity and temperature.

$$\mu = A\exp^{(\frac{E_\mu}{RT})} \text{---------- [Eq. 29]}$$

However, when a sudden change occurs in the structure of the liquid melt, this straight line relationship is lost reflecting the structural dependence of viscosity in addition to the effect of temperature on it raising the temperature of the melt, the following may happen:

i. The cation – anion bond may be weakened.
ii. Anions may breakdown gradually so that smaller anions, i.e. flow units are generated.

On account of the above, the activation energy of viscous flow may remain the same ('i' above) or it may also change along with the change in temperature. It is proposed by Mills [74] the NBO/T is more effective in as a measure of de-polymerization of the silicate melts though Λ_{cor} can do the job better for non – silicate melts. It has to be born in mind that the degree of polymerization of a silicate melt is the most important factor which affects the physical properties of the melt such as viscosity, conductivity, flow characteristics, etc.

2.4.2 Ionic Interaction and Viscosity of Silicate Melts

Considering viscosity as a reaction–rate–phenomenon, it can be presented by the following equation.

$$\mu = \frac{Nh}{V}\exp^{(-\frac{\Delta S^*}{R})}\exp^{(\frac{\Delta H^*}{RT})} \text{ ---------- [Eq. 30]}$$

Where N is the Avogadro's number, h is the Planck's constant, v is the molar volume and S is the entropy. Here, ΔH^* is influenced by the average flow unit size and the number and extent of various columbic interactions between the flow units and the associated species present in the melt. These columbic interactions can be categorized as follows:

a) Between singly bonded oxygen of the flow units and the metallic ions (M^{++}- O^- type) and

b) Between two singly bonded oxygen of two different flow units (O^- - O^- type).

Greater the number of 'a' type interactions obviously greater is the ΔH^* value. However, it must be noted that O^- - O^- type interactions being repulsive, would tend to decrease the ΔH^* value. Greater will be the attractive interactions lesser will be 'S' the entropy and hence higher will be the ΔH^* value. For similar reasons, repulsive interactions will tend to decrease ΔH^*.

With increased metal oxide percentage, the flow units become smaller and smaller and the volume of one mole of anionic units present in the melt (v), decreases. From the equation [Eq. 30]:

$$\mu = \frac{Nh}{V} \exp^{(-\frac{\Delta S^*}{R})} \exp^{(\frac{\Delta H^*}{RT})}$$

It must be understood that the variation of ΔS^* and 'v' tend to counter the effect due to variations in ΔH^*. However, since it is obvious that viscosity decreases with increasing additions of metal oxides, the effects of ΔH^* variations bringing in the change in viscosity seem to be more dominating compared to that due to ΔS^* and/or 'v'.

We have, thus discussed the effect of structure of the liquid slag on viscosity of binary, ternary and some complex silicate melts. We now make an attempt at discussing a system of greater industrial importance, the blast furnace slag. However, it will be more pertinent to note the following prior to facing up the case of the blast furnace slag. The system of liquid slags containing $CaO–MgO–Al_2O_3–SiO_2$ type melts are of greater practical

importance. These are also the primary constituents of a blast furnace slag melt, which may also contain some alkaline earth oxides. The viscosities of these systems have been thoroughly studied and reported [63, 76-78]. It is established that the effect of alumina on the viscosity of the melt is as great as that of silica. Also is it reported from the above studies that of constant lime content, the viscosity of the melt decreases with increasing magnesia (MgO) content when the silica content is also constant. They further report that at constant Al_2O_3 and SiO_2 contents increasing MgO content (up to 10 wt %) decreases the viscosity. Similar findings have been reported [79] in case of synthetic slags containing 40-48% CaO, 17.5-40% Al_2O_3, 15-30% SiO_2 and 4-12% MgO. Alkaline earth oxides are interchangeable in their effects on the viscosity of binary as well as quaternary melts [44, 60]. This has been illustrated in the Fig. 2.6 given below.

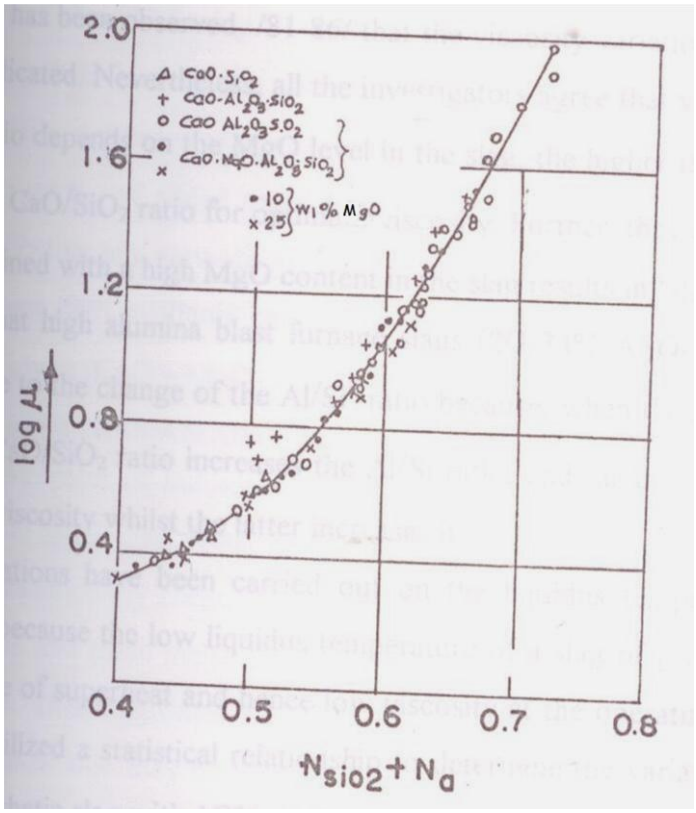

Fig 2.6. Variation of viscosity with composition of CaO-MgO-Al_2O_3-SiO_2 melts at 1500^{o}C [26].

The Fig. 2.6 illustrates that CaO and MgO are replicable on the molar basis. Also it is evident from the Fig. 2.6 that the viscosity data on binary, ternary and quaternary melts could be represented by a single curve with only a small scatter. However, a variation of upto 20% in viscosity values is observed for the same Na + N_{SiO2} value which limits the usefulness of this curve. In addition it is interesting to note that MgO is actually amphoteric in nature and that like all amphoteric oxides, the strength of MgO as a basic oxide increases with decreasing density of the melt [80]. This is evident from the fact that in the CaO –SiO_2– MgO system, MgO behaves similarly as CaO but in the Na_2O–SiO_2–MgO system it acts as an acidic oxide.

2.4.3 Viscosity of Blast Furnace Slags

CaO, SiO_2, Al_2O_3 and MgO are the major constituents of the blast furnace slag which may also contain MnO, FeO, CaO and sometimes TiO_2 as the minor constituents. CaO/SiO_2 represents the basicity of the blast furnace slag which may also be presented as the ratio of the amount of basic oxides to that of the acid oxides. Al_2O_3 in these slags may behave as an amphoteric oxide depending on the slag composition.

The viscosity variation of the blast furnace slags with the change of composition is complicated [16, 81-85]. However, it is generally agreed that:

a) For the blast furnace slag the viscosity variations with the variation of C/S (CaO/SiO_2) ratio is a function of the MgO content of the slag.
b) The higher is the MgO content; the lower is the desired C/S ratio for optimum viscosity values.
c) Al_2O_3 is responsible for erratic viscosity values of the blast furnace slag. At constant Al_2O_3 contents with an increase in the CaO/SiO_2, Al/Si ratio increases. An increased

ratio of CaO/SiO_2 decreases the slag viscosity whereas an increased Al/Si ratio increases it.

2.4.4 Flow characteristics of Blast Furnace Slags

According to German Standards 51730 fusion behavior or flow characteristics of the blast furnace slag is expressed in terms of four characteristics temperatures. The process of determination for these characteristics temperatures consists in studying a small cube – shaped representative sample to the effects of gradually increasing heat input. The shape changes of this cube – shaped sample as consequence of heating to gradual elevated temperatures is observed continuously through a microscope and based on this shape changes the characteristics temperature representing the fusion behavior of the slag are expressed.

Initial Deformation Temperature (IDT)

At this temperature the first rounding up of the edges of the cube – shaped sample focus plane. This is, thus the temperature of which the first sign of the change of shape of the sample is seen. This initial change in shape indicates the beginning of sintering of the test specimen. Rheologically this temperature symbolizes the surface stickiness of the slag.

Softening Temperature (ST)

At this temperature the outline of the shape of the test specimen starts changing. This is the temperature at which the test specimen shrinks by one division on the measuring scale. In other words this is the temperature at which the distortion of the sample begins. Rheologically this temperature symbolizes the start of plastic distortion.

Hemispherical Temperature (HT)

This temperature also represents the fusion point of liquidus temperature of the sample. At this temperature the cube shaped test specimen is fused down to a hemispherical shape. At this temperature the height of the specimen is equal to half of its basic length. Rheologically this temperature symbolizes sluggish flow of the slag.

Flow Temperature (FT)

This is the temperature at which the specimen liquefies. It is reported as the temperature at which the height of the specimen is equal to one third of the height it had at the hemispherical temperature. Rheologically this temperature symbolizes the liquid mobility of the slag.

For all practical purposes, it is to be clearly understood that the fusion behavior of the non – metallic melts, when a pyro-metallurgical process is carried out in a furnace is more important than the exact liquidus temperature. It is because the liquidus temperature indicates the extent of extra heat at a given temperature which may have a say on the viscosity and hence on the reaction rates in the furnace. However, in the blast furnace operation in particular, it is necessary to have a narrow softening – melting range than a sharp low liquidus temperature. When this difference is small, the slag is formed as a 'short' slag. Such a slag, when it melts does not use more thermal energy for its flow. It trickles down the solid burden exposing fresh interfaces for an enhanced rate of reaction. On the other hand, when the difference is large the slag is formed as a 'long' slag. Such a slag, after is rendered molten, required higher thermal energy for its easy flow.

Much work has not been done in respect of the fusion behavior of the blast furnace slag. However, it is established that this phenomenon concerning the blast furnace slag depends squarely on the composition of the slag. It has been reported [16, 81-85] that a high CaO/SiO_2 ratio combined with a high MgO content in the slag results in a 'short' slag. The compositional dependence of alumino-thermic ferrochrome slags has been reported by Sahoo et al [31] while the same authors have developed statistical equations to predict the fusion behaviors of the blast furnace slag [86]. Dash et al. [14] has also carried out extensive work to report the composition – dependence of blast furnace slag when its fusion behavior is concerned. They have reported that:

- A high C/S ratio is beneficial for the blast furnace process as it ensures the formation of a ‘Short Slag’. In their study, the C/S ratio value was in the range of 0.93 to 1.09 while MgO content was in the range of 6.5 to 11.01 wt.% and Al_2O_3 content was approximately 20 wt.%.
- Increased MgO content combined with a high C/S ratio form ‘Short Slags’ which is advantageous to blast furnace process.

3. Experimental Details

3.1 Material and Sample Preparation

Twenty five numbers of random slag samples collected from different operating blast furnaces in the country over a period of about six months constitute the chief materials for the present study. The chemical compositions of these samples are determined in the laboratory adopting the analytical method. The compositional detail of these samples is provided in Table 3.1. The viscosities of all the slags are estimated using the models, briefly discussed and presented subsequently in section 3.2.

Table 3.1. Composition (in wt. %) of BF slag collected from different Indian industries.

Sl. No.	Al_2O_3	CaO	MgO	SiO_2	Na_2O	K_2O	Fe_2O_3	TiO_2	MnO	CaO/SiO_2
Slag 1	19.04	34.57	6.51	36.72	-----	-----	-----	-----	-----	0.94
Slag 2	13.80	35.11	9.57	36.50	-----	-----	2.52	0.80	-----	0.96
Slag 3	16.95	36.06	9.09	36.58	0.07	0.10	0.24	0.22	-----	0.99
Slag 4	18.07	34.15	6.50	34.06	-----	-----	-----	-----	-----	1.00
Slag 5	16.76	36.95	7.66	36.49	0.01	0.19	1.38	0.10	-----	1.01
Slag 6	20.28	32.55	10.40	31.58	-----	-----	0.74	0.76	-----	1.03
Slag 7	17.90	36.20	7.05	34.60	-----	-----	-----	-----	-----	1.05
Slag 8	16.58	36.20	9.57	34.32	1.36	0.82	0.53	0.55	0.055	1.05
Slag 9	20.05	33.61	10.09	32.05	-----	-----	0.62	0.82	-----	1.05
Slag 10	19.00	34.04	10.09	32.05	-----	-----	1.02	0.70	-----	1.06
Slag 11	21.97	34.12	8.87	32.00	-----	-----	1.08	0.80	-----	1.07
Slag 12	19.00	33.40	10.40	31.30	-----	-----	3.70	0.70	-----	1.07
Slag 13	20.58	33.70	9.58	30.92	-----	-----	-----	-----	-----	1.09
Slag 14	18.77	35.10	10.40	32.24	-----	-----	0.92	0.76	-----	1.09
Slag 15	17.45	35.03	11.11	31.80	2.54	0.92	0.60	0.50	0.055	1.10
Slag 16	17.56	34.97	11.75	31.90	2.12	0.82	0.53	0.175	0.084	1.10
Slag 17	17.00	35.78	11.88	32.48	1.10	0.52	0.60	0.55	0.051	1.10
Slag 18	16.31	36.84	10.56	33.25	1.10	0.52	0.54	0.82	0.055	1.11
Slag 19	17.66	38.93	7.52	32.60	0.05	0.09	0.47	0.30	-----	1.19
Slag 20	16.92	38.00	10.23	31.86	0.98	0.48	0.66	0.70	0.050	1.19
Slag 21	17.04	36.96	11.22	31.08	1.80	0.88	0.40	0.50	0.053	1.19
Slag 22	17.32	37.70	10.89	30.77	2.00	0.52	0.45	0.20	0.072	1.23
Slag 23	16.73	38.80	9.74	30.87	-----	-----	1.40	0.40	-----	1.26
Slag 24	20.57	37.55	8.82	26.77	0.08	0.14	1.97	0.25	-----	1.40
Slag 25	20.89	43.25	11.01	30.84	-----	-----	0.44	0.70	-----	1.40

Sampling for different analysis is usually done in two steps: coning and quartering. In coning and quartering the sample is first powdered and placed on a clean surface in the form of a cone like heap. The cone is then spread out into a circular, flat cake [26]. The cake is then divided radically into quarters and two opposite quarters are combined. The other two quarters are discarded. The process is repeated as many times as necessary to obtain the quantity desired for some final use (e.g. as the laboratory sample or as the test sample). If the process is performed only once, coning and quartering is no more efficient than taking alternate portions and discarding the others.

3.2. Mathematical Models for Prediction of BF Slag Viscosity

3.2.1. Urbain Model [87]

The model is based on CaO-Al_2O_3-SiO_2 system. In this model the slag constituents are classified into three categories: glass formers (X_G), network modifiers (X_M) and amphoterics (X_A).

$$X_G = X_{SiO_2} + X_{P_2O_5} \text{---------- [Eq. 31]}$$

$$X_M = X_{CaO} + X_{MgO} + 3X_{CaF_2} + X_{FeO} + X_{MnO} + X_{CrO} + X_{NiO} + X_{Na_2O} + X_{K_2O} + X_{Li_2O} + 2X_{TiO_2} + 2X_{ZrO_2} \text{---------- [Eq. 32]}$$

$$X_A = X_{Al_2O_3} + X_{Fe_2O_3} + X_{B_2O_3} + X_{Cr_2O_3} \text{---------- [Eq33]}$$

This model takes into consideration of Weymann-Frenkel relation for calculation of viscosity. According to Weymann-Frenkel:

$$\text{Viscosity, } \eta = A T \exp\left[\frac{1000B}{T}\right] \text{---------- [Eq. 34]}$$

Where A and Bare compositionally dependent parameters, and

$$-\ln A = mB + n \text{---------- [Eq. 35]}$$

Where, m and n are empirical parameters.

Urbain found that A and B can be linked through the following equations:

$$-\ln A = 0.29B + 11.57$$ ---------- [Eq. 36]

And

$$B = B_0 + B_1 X_G^* + B_2 (X_G^*)^2 + B_3 (X_G^*)^3$$---------- [Eq. 37]

$$B_0 = 13.8 + 39.9355\alpha - 44.049\alpha^2$$ ---------- [Eq. 38]

$$B_1 = 30.481 - 117.1505\alpha + 139.9978\alpha^2$$ ---------- [Eq. 39]

$$B_2 = -40.9429 + 234.0486\alpha - 300.04\alpha^2$$---------- [Eq. 40]

$$B_3 = 60.7619 - 153.9276\alpha + 211.1616\alpha^2$$---------- [Eq. 41]

$$\alpha = X_M^*/(X_M^* + X_A^*)$$---------- [Eq. 42]

This model works mainly on the basis of M_XO and so this creates extra ions. In order to normalise X_G, X_M& X_A, each of them is divided by the term ($1+ X_{CaF2}+ X_{TiO2} + X_{ZrO2}$) to give X_G*, X_M*&X_A*.

3.2.2. Urbain-I Model [87]

Urbain modified the model to calculate B values for modifiers CaO, MgO and MnO individually. B values for each of the modifier CaO, MgO and MnO can be calculated from the equations:

$$B_i = a_i + b_i\alpha + c_i\alpha^2$$ ---------- [Eq. 43]

Where, the a_i, b_i and c_i values are given in Table 3.2.

After finding the B values for each modifier then B values for each modifier can be calculated from equation 7.

Total B can be calculated from the equation:

$$B_{global} = (X_{CaO}B_{CaO} + X_{MgO}B_{MgO} + X_{MnO}B_{MnO})/(X_{CaO} + X_{MgO} + X_{MnO})$$---------- [Eq 44]

Table 3.2.Values of a_i, b_i and c_i used in Urbain - I model [87].

	a_i	b_i			c_i		
i	all	Mg	Ca	Mn	Mg	Ca	Mn
0	13.2	15.9	41.5	20.0	-18.6	-45.0	-25.6
1	30.5	-54.1	-117.2	26	33.0	130.0	-56.0
2	-40.4	138	232.1	-110.3	-112.0	-298.6	186.2
3	60.8	-99.8	-156.4	64.3	97.6	213.6	-104.6

3.2.3. Urbain Modified Model [88]

This model is also based on the Weymann-Frenkel equation and is applied for SiO_2-Al_2O_3-CaO-FeO system. According to this model constant value of *m* and *n* in Eq. (5) proposed by Urbain can't provide an accurate description of "experimental" values of *A* and *B* over the whole compositional range.In this model A and B could be achieved with a constant *n* and the following equation for m:

$$m = m_A X_A + m_C X_C + m_F X_F + m_S X_S \text{---------- [Eq. 45]}$$

Where,m_A,m_C, m_F and m_S are model parameters, and X_A,X_C,X_F and X_S are the molar fractions of Al_2O_3, CaO, FeO and SiO_2 respectively.

$$B = \sum_{i=0}^{3} b_i^0 X_S^i + \sum_{i=0}^{3}\sum_{j=1}^{2}[b_i^{c,j}(\frac{X_C}{X_C+X_F}) + b_i^{F,j}(\frac{X_F}{X_C+X_F})]\alpha^j X_S^i \text{---------- [Eq. 46]}$$

$$\text{And } \alpha = \frac{X_C+X_F}{X_C+X_F+X_A} \text{---------- [Eq. 47]}$$

Where, b_i^0 values are parameters for the Al_2O_3-SiO_2 system. $b_i^{c,j}$ and $b_i^{F,j}$ are sets of parameters for CaO and FeO respectively. The values of n, $m_i$and $b_i^j$are given in Table 3.3.

Table 3.3. Values of n, $m_i$and b_i^jused in modified Urbain model [88].

	j/i	0	1	2	3		
b_i^0	0	13.31	36.98	-177.70	190.03	n	9.322
$b_i^{c,j}$	1	5.50	96.20	117.94	-219.56	m_F	0.665
	2	-4.68	-81.60	-109.80	196.00	m_c	0.587
$b_i^{F,j}$	1	34.30	-143.64	368.94	-254.85	m_A	0.370
	2	-45.63	129.96	-210.28	121.20	m_S	0.212

3.2.4. Ray& Pal Model [9,10]

It uses Weymann-Frenkel equation as follows:

Viscosity, $$\eta(\mathrm{p}) = \mathrm{AT}e^{(\frac{1000B}{T})}$$ ---------- [Eq. 48]

Where A and B can be calculated as:

$$-\ln\mathrm{A} = 0.2056\mathrm{B} + 12.492$$ ---------- [Eq. 49]

$$\mathrm{B} = 297.14\Lambda^2 - 466.69\Lambda + 196.22$$ ---------- [Eq. 50]

Λ is the optical basicity and is calculated by the following equation:

$$\Lambda = \frac{\sum \mathrm{X_i n_i \Lambda_i}}{\sum \mathrm{X_i n_i}}$$ ---------- [Eq. 51]

Where, Xis the mole fraction, n is the number of oxygen atoms in the molecule and $\Lambda_i$is the optical basicity of the components [9, 10, 89, 90]. The optical basicity (Λ) is defined as below:

$$\Lambda = \frac{\text{Electron donor power of slag}}{\text{Electron donor power of CaO}}$$ ---------- [Eq. 52]

3.2.5. NPL Model [9, 89]

The NPL (National Physical Laboratory) model was developed by Mills and Sridhar which is based on Arrhenius equation. It relates the viscosity of slag to the structure through the optical basicity.

The viscosity can be calculated by:

$$\eta(\mathrm{pa.s}) = \mathrm{A}e^{(\frac{B}{T})}$$ ---------- [Eq. 53]

and A and B can be calculated by:

$$\ln\left(\frac{\mathrm{B}}{1000}\right) = -1.77 + (2.88/\Lambda)$$ ---------- [Eq. 54]

$$\ln\mathrm{A} = -232.69\Lambda^2 + 357.32\Lambda - 144.17$$ ---------- [Eq. 55]

3.2.6. Iida Model [11-13]

Iida's viscosity model is based on the Arrhenius type of equation. It takes into account by using basicity index B_i.

$$\eta(\text{pa.s}) = A\eta_0 \exp(\frac{E}{B_i}) \text{ ---------- [Eq. 56]}$$

Where A is pre-exponential term, E is the activation energy and η_0 is hypothetical viscosity for each slag constituent. The parameters A, E and η_0 are all given as functions of temperature:

$$A = 1.745 - 1.962 \times 10^{-3}T + 7.000 \times 10^{-7}T^2 \text{ ---------- [Eq. 57]}$$

$$E = 11.11 - 3.65 \times 10^{-3}T \text{ ---------- [Eq. 58]}$$

$$\eta_0 = \sum \eta_{0i} X_i \text{ ---------- [Eq. 59]}$$

η_{0i} values can be calculated by:

$$\eta_{0i} = 1.8 \times 10^{-7} \left[\frac{(M_i T_{mi}^2)^{\frac{1}{2}} \exp\left(\frac{H_i}{RT}\right)}{V_{mi}^{\frac{2}{3}} \exp\left(\frac{H_i}{RT_{mi}}\right)} \right] \text{ ---------- [Eq. 60]}$$

Where, M_i molecular weight, V_{mi} molar volume, T_{mi} melting temperature, R gas constant, X mole fraction and H_i melting enthalpy of individual component i. H_i can be calculated from a simplified formula:

$$H_i = 5.1 T_{mi}^{1.2} \text{ ---------- [Eq. 61]}$$

In this model the basicity index B_i is calculated by:

$$B_i = [\sum(\alpha_i W_i)_B / \sum(\alpha_i W_i)_A] \text{ ---------- [Eq. 62]}$$

Where, α_i is specific coefficient and W_i mass percentage for component i. The subscripts *A* and *B* represent acidic oxide and basic oxide respectively. Various constituents are divided into the following categories:

(1) Acidic (SiO_2, ZrO_2, and TiO2) denoted by subscript A.

(2) Basic (CaO, MgO, Na_2O, K_2O, Li_2O, FeO, MnO, CrO, CaF_2, etc.) denoted by subscript B.

(3) Amphoteric (Al_2O_3, B_2O_3, Fe_2O_3, Cr_2O_3).

3.2.7. Iida Modified Model [11-13]

The Iida model was modified so as to take into consideration the amphoterics. Their basicity changed according to the temperature. It was found that Fe_2O_3 and Cr_2O_3 behaved as basic oxides. Hence, they are placed in the numerator. The basicity index formula was modified as shown below:

$$B_i = \left[\sum(\alpha_i W_i)_B + \alpha^*_{Fe_2O_3} W_{Fe_2O_3} + \alpha^*_{Cr_2O_3} W_{Cr_2O_3}\right] / \left[\sum(\alpha_i W_i)_A + \alpha^*_{Al_2O_3} W_{Al_2O_3}\right] \text{ --- [Eq. 63]}$$

Where, α_i^* is the modified specific coefficient indicating the interaction of the amphoteric oxide with other components in slag. If α* is independent of slag composition and temperature, then $\alpha_i^* = \alpha_i$.

$$\alpha^*_{Al_2O_3} = aB_i + bW_{Al_2O_3} + c \text{ ---------- [Eq. 64]}$$

Where a, b and c are given as:

$$a = 1.20 \times 10^{-5}T^2 - 4.3552 \times 10^{-2}T + 41.6 \text{ ---------- [Eq. 65]}$$

$$b = 1.40 \times 10^{-7}T^2 - 3.4944 \times 10^{-4}T + 0.2062 \text{ ---------- [Eq. 66]}$$

$$c = -8.00 \times 10^{-6}T^2 + 2.5568 \times 10^{-2}T - 22.16 \text{ ---------- [Eq. 67]}$$

3.3. High Temperature Viscometer

The viscosities of some selected slags (Slag 5, Slag 18, Slag 21 and Slag 24)[1] are measured experimentally using high temperature viscometer, model VIS 403 HF supplied by BAHR, Germany. A schematic of the viscometer is shown in Fig. 3.1. This viscometer is an inner cylinder rotating type where dynamic viscosity is calculated by the measurement of torque of a rotor immersed in the slag melt.

[1] To avoid the measurement difficulties, the viscosities of some selected slag samples are measured experimentally. The selection is made based on the slag composition pertaining to C/S ratio.

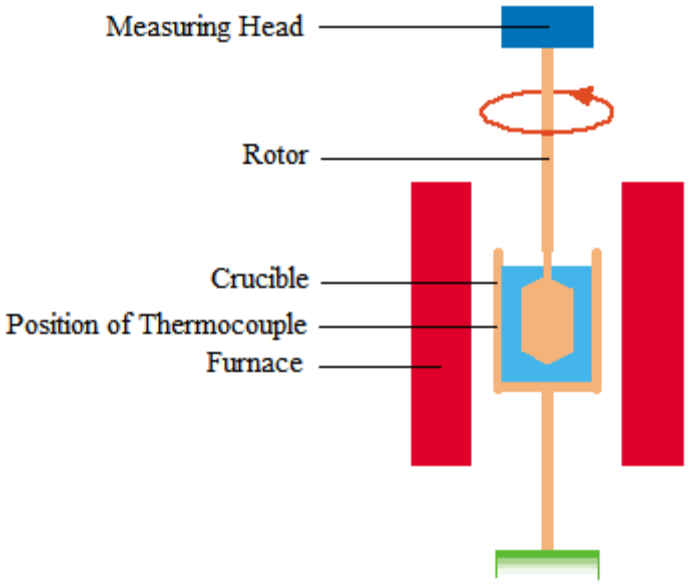

Fig. 3.1. Schematic diagram of high temperature viscometer, model VIS 403 HF.

3.4. Heating Microscope

A Leitz heating microscope, with a Leica camera and 1750^{o}C furnace as a supplementary attachment has been used in the present work to determine the flow characteristics of the slag samples. A schematic diagram of the assembly is presented in Fig. 3.2. In the present investigation in order to avoid any likely reactions with the atmosphere and/or the recrystallized alumina sample holder Argon gas is introduced into the furnace throughout the entire period of measurement and also a platinum holder is used in place of the recrystallized alumina sample holder. The heating rate adopted is 8 ^{o}C/min maximum up to 900 ^{o}C and 2 – 4 ^{o}C/min maximum beyond 900 ^{o}C. Regular photographs are taken to record the readings. Two readings are taken per sample. If the readings differ by more than 10^{o}C the results are rejected; if not the average of the two readings is reported. The characteristic temperatures are measured by noting the specific shape changes undergone by the slag samples as a consequence of the deformation caused on heating the same. These shape changes are specific to the sample at a specific temperature as observed continuously

during heating in a heating microscope. ST, the softening temperature, is the temperature at which the outline of the cube-shaped sample specimen starts changing and it is reported as the temperature at which the specimen shrinks by one division on the grid pattern. HT, the hemispherical temperature, is the temperature at which the sample fuses down to a hemispherical shape and is measured as the temperature at which the height of the specimen becomes equal to half of its base length. And FT, the flow temperature, is the temperature at which the specimen liquefies and is reported as the temperature at which the height of the specimen is equal to one-third of the height it had at hemispherical temperature. Fig. 3.3 presents these specific shapes of the sample at specific characteristic temperature presented below each of the photographs as obtained directly from the instrument during experimentation.

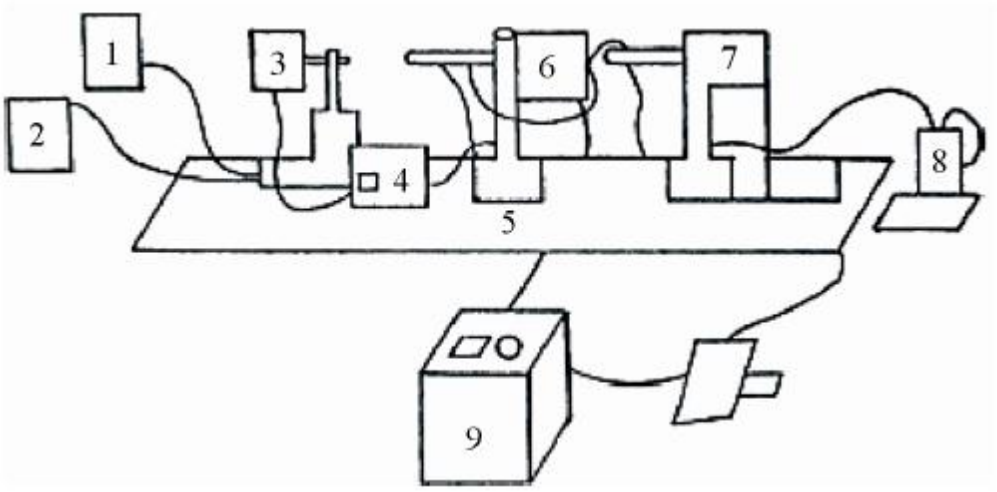

Fig.3.2. Line diagram of the hot stage microscope used in the present study [26].

1. Cooling water tank; 2. Cooling water re-circulating tank; 3. Light source; 4. Regulating transformer for light source; 5.Optical bench; 6.High temperature electrical furnace with specimen carriage; 7.Observation and photo microscope; 8. Digital thermometer; 9. Regulating transformer for high temperature electrical furnace.

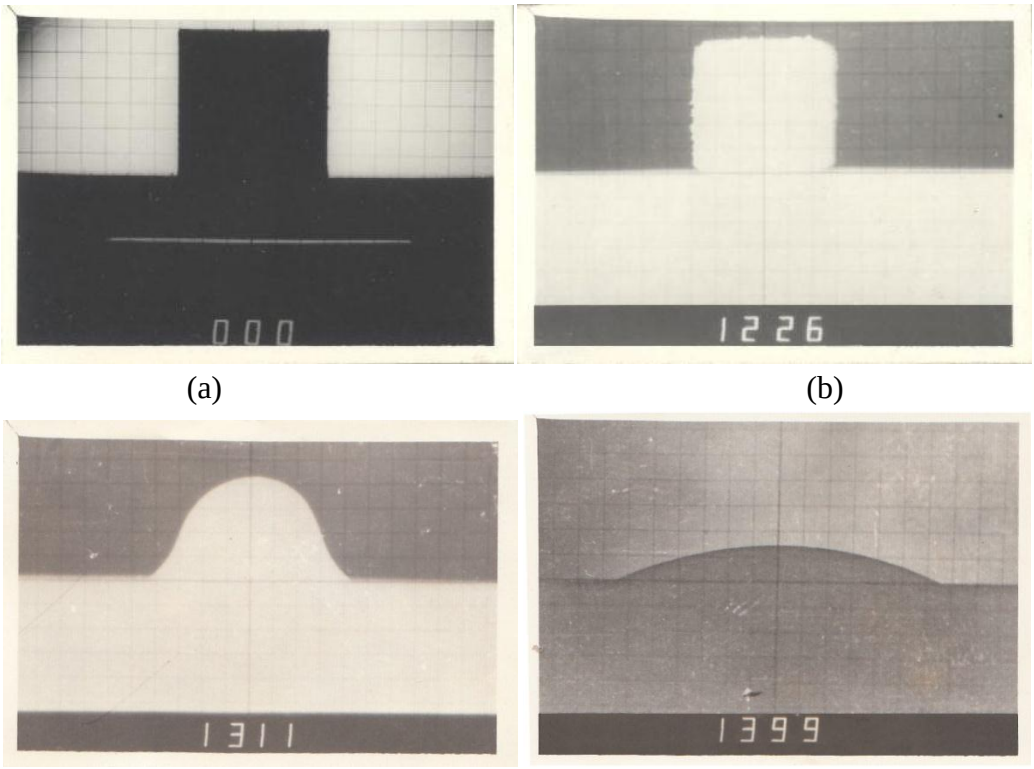

(a) (b)

(c) (d)

Fig.3.3. Photographs illustrating the characteristic temperatures of a slag owing to its shape change on deformation as a consequence of heating: (a) Original shape of the sample, (b) ST, the Softening Temperature in ^{o}C, (c) HT, the Hemispherical Temperature in ^{o}C and (d) FT, the Flow temperature in ^{o}C.

3.5. X-Ray Diffraction (XRD)

XRD is carried out in a Panalytical X-Pert Pro system with Cu target. To observe the crystalline phases in the slag samples, the samples are subjected to slow cooling @ 5˚C/min from 1400˚C to 200˚C (soaking at 1400˚C/1 hour) and then from 200˚C to room temperature samples cooled overnight in the furnace. It may be noted that some selected slag samples are observed for XRD analysis. The Slag 1, Slag 4, Slag 9, Slag 14, Slag 22 and Slag 24 are analyzed in XRD.

3.6. Optical Microscopy

Optical microstructures are obtained in a Leitz universal microscope under reflected light. Again some selected slag samples (Slag 4, Slag 12, Slag 17 and Slag 19) are analysed for microscopic study. The selection is made with the objective to show different phases in the slag samples. As dominant phases are equivalent in most of the samples, only four slag samples are represented in this report. The quenched samples are metallographic polished using standard steps [26] and microstructures are obtained on the polished surfaces without any etching treatment. The photo micrographs were taken on polished surface under reflected light optical microscope. Refractive index has been found out which are different for different phases. Also pleochroism has been taken in to consideration to identify different phases. As tetragonal coloured minerals are dichroic and monoclinic minerals are trichroic. These samples are also chemically etched with HF where different minerals takes different colour based on basicity and silica content. For example Merwinite takes yellowish red colour. Observation of refractive index, pleochroism, colour after etching and more over comparison with standard phases, different phase are identified under reflected light.

4. Results and Discussion

4.1. Viscosity

The viscosity values of all the slags, as estimated by different viscosity models, are presented in Fig. 4.1 – viscosity being plotted against temperature. Fig. 4.2 presents the viscosity of the slags measured by high temperature viscometer. It may be observed that the viscosities measured by high temperature viscometer are best fitted with the viscosities that are obtained by using the Iida model.

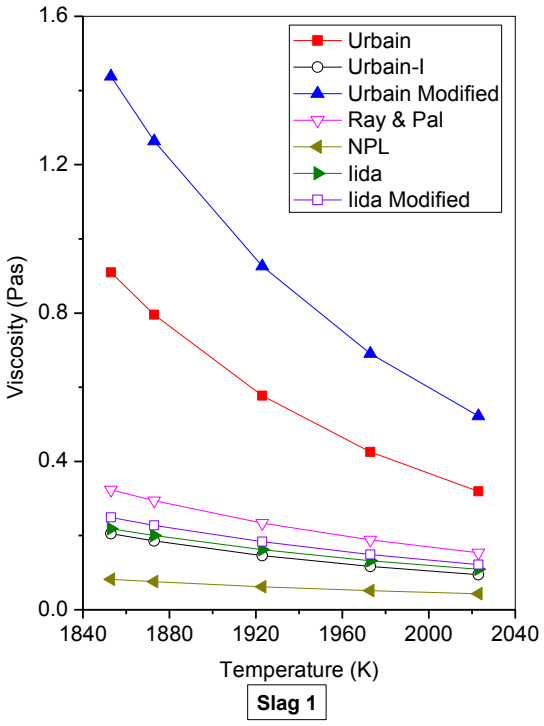

Slag 1

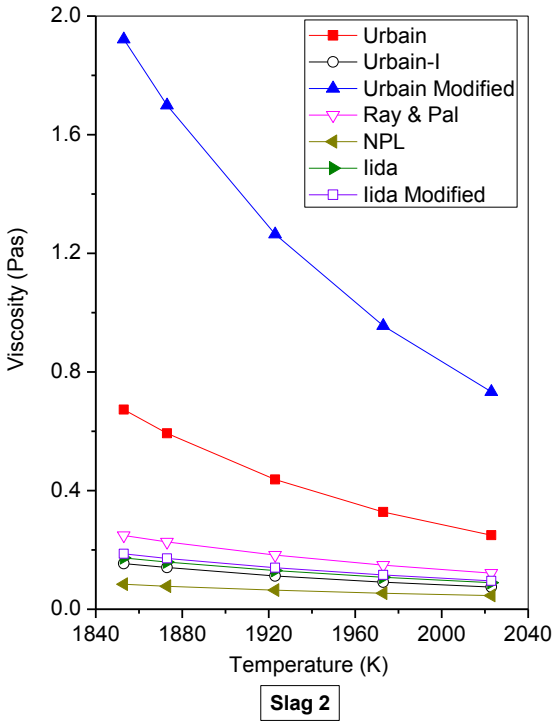

Slag 2

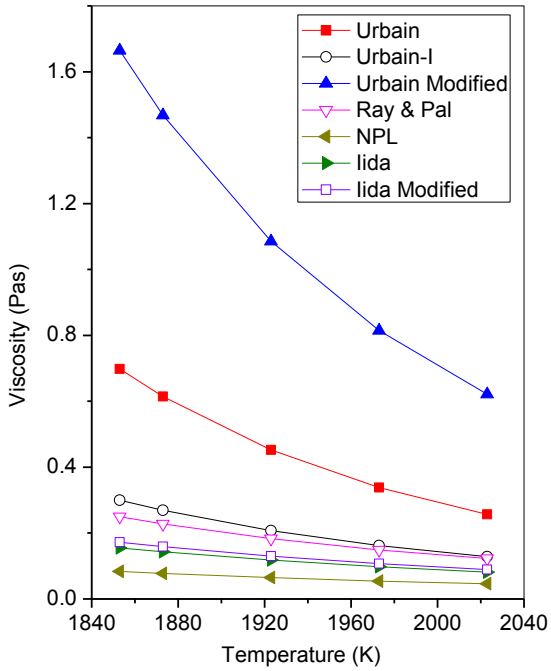

Slag 3

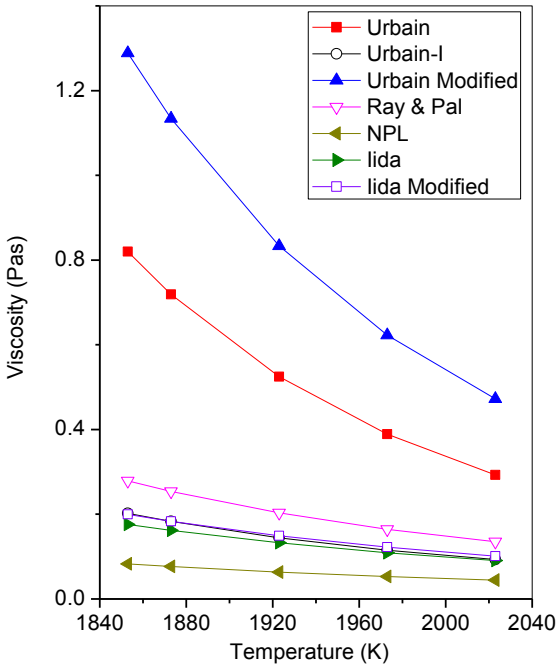

Slag 4

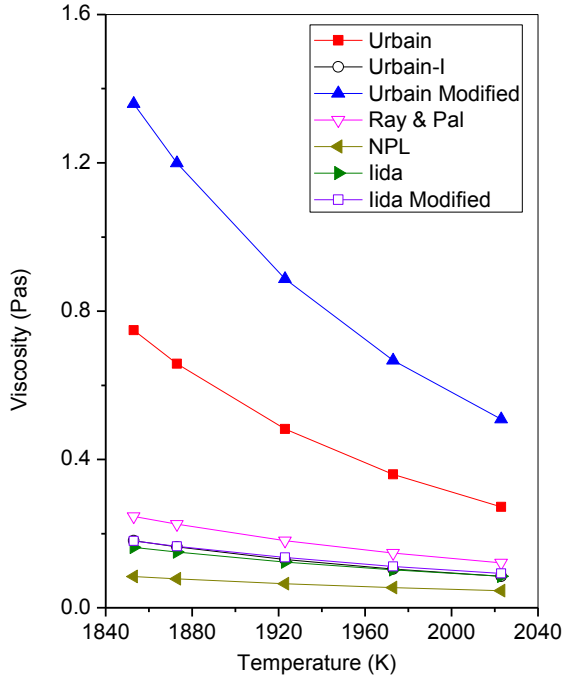

Slag 5

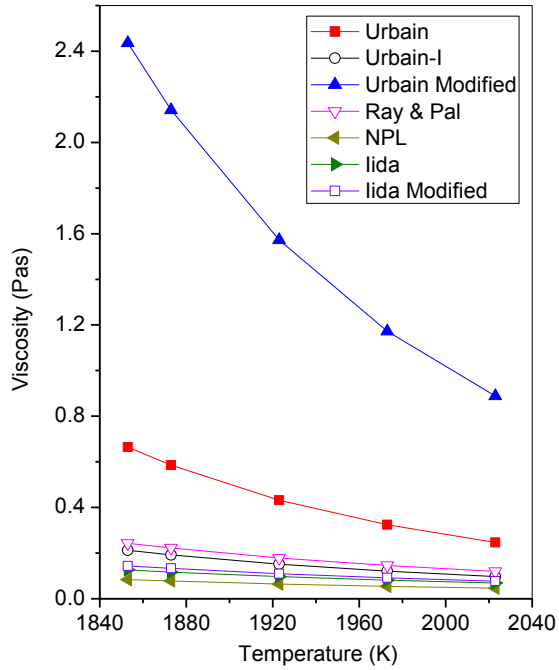

Slag 6

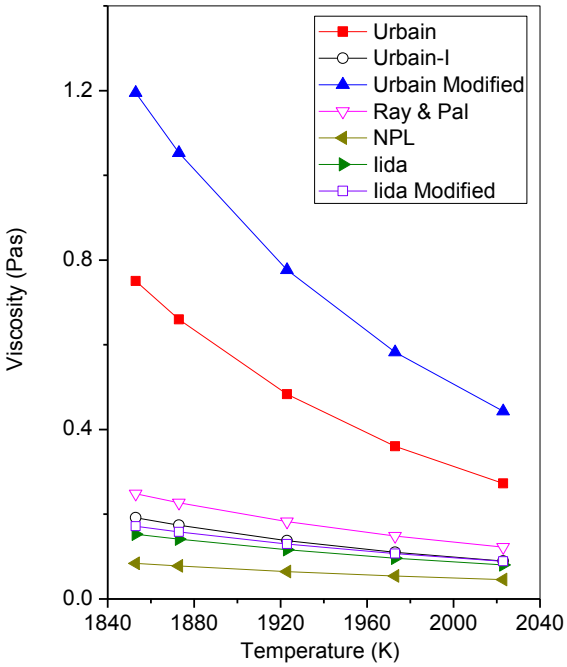

Slag 7

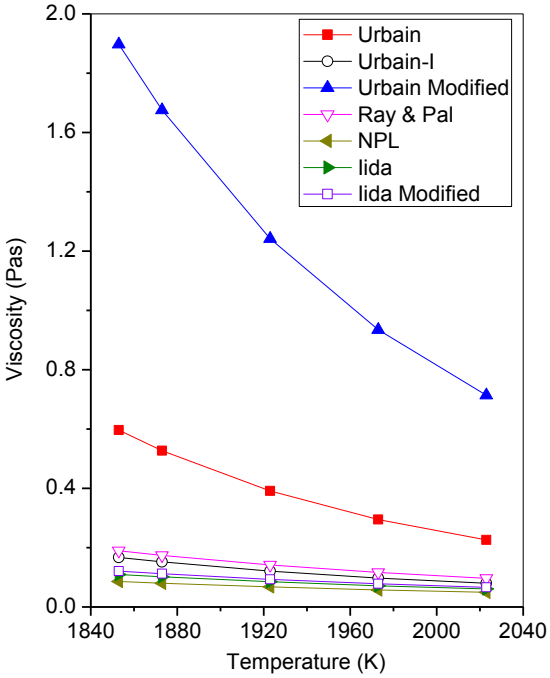

Slag 8

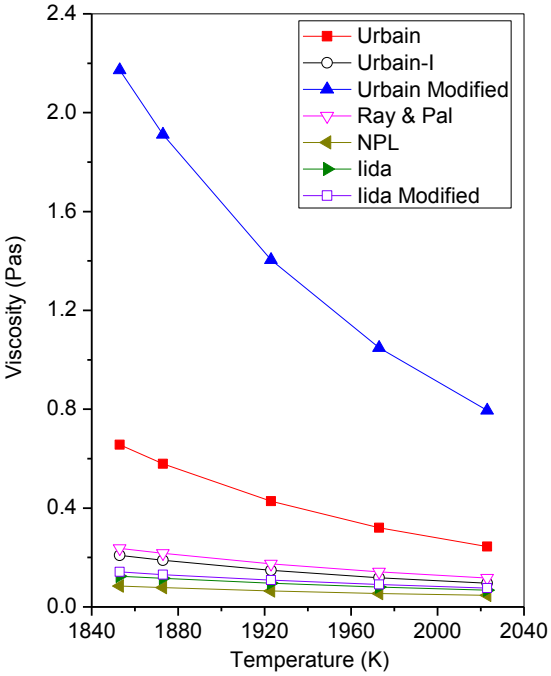

Slag 9

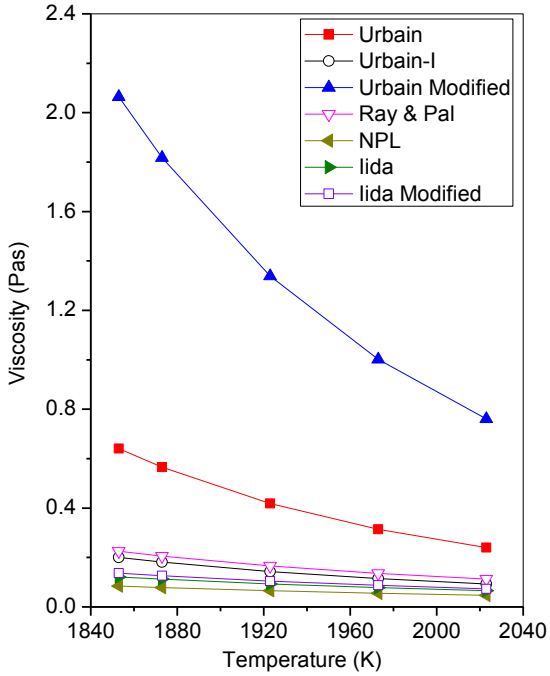

Slag 10

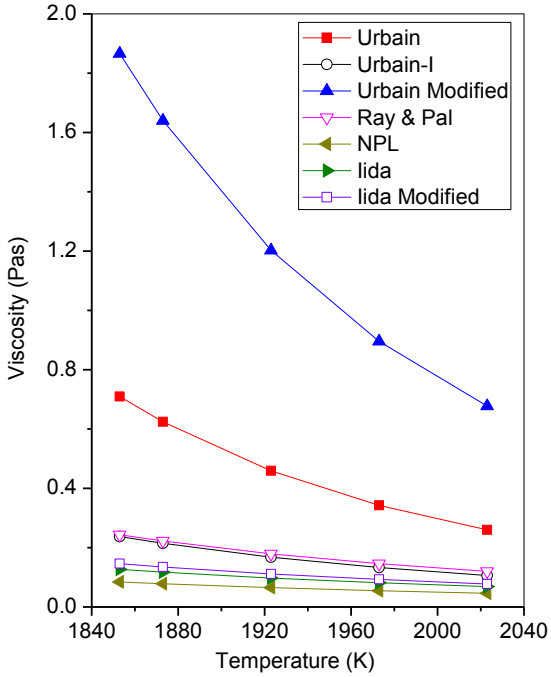

Slag 11

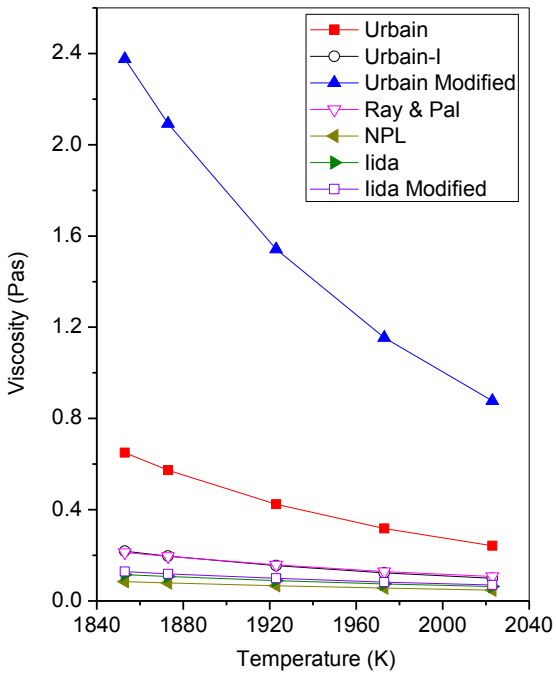

Slag 12

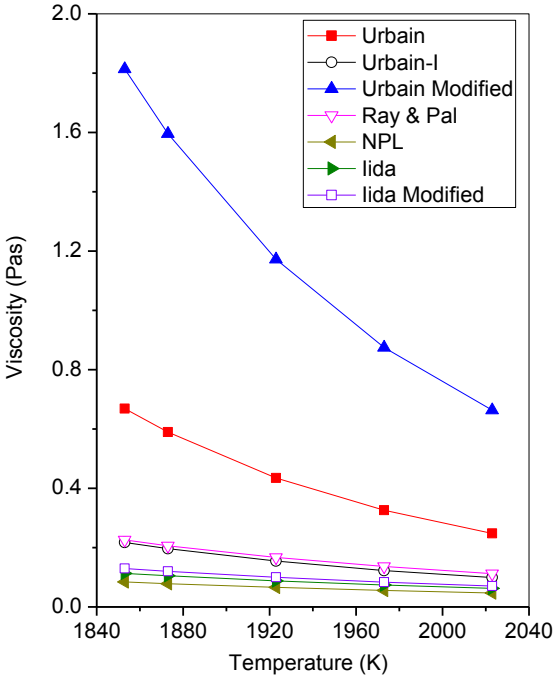

Slag 13

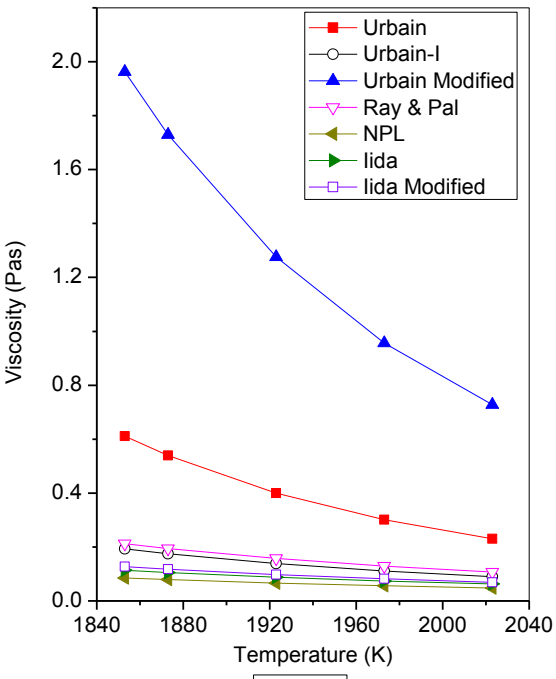

Slag 14

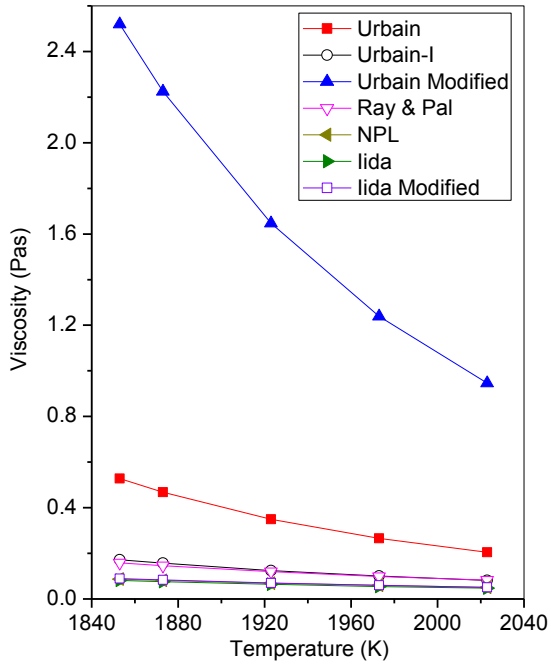

Slag 15

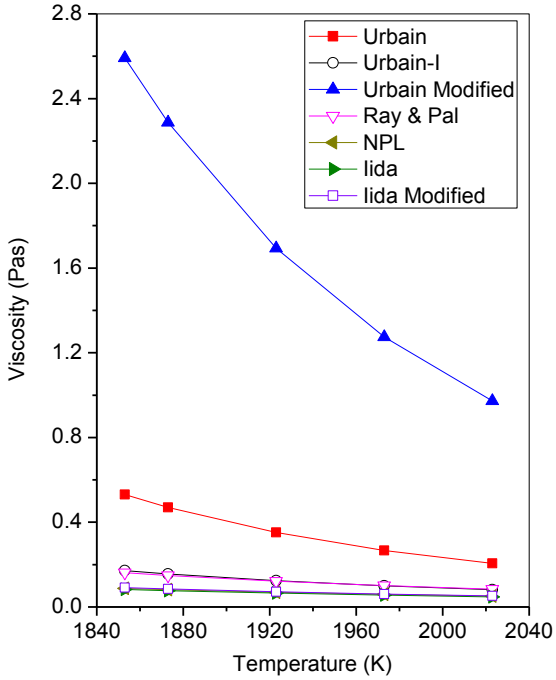

Slag 16

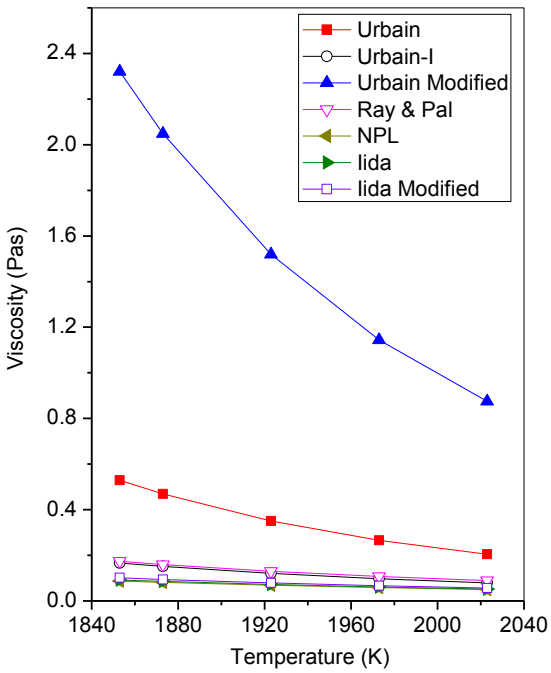

Slag 17

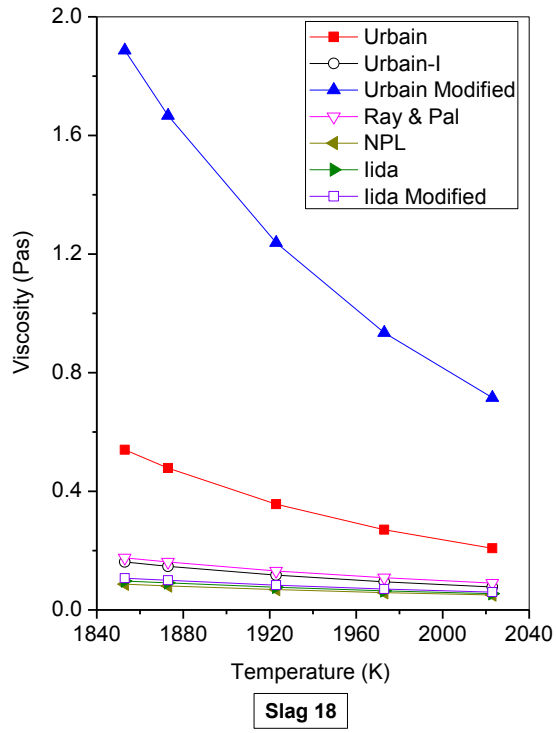

Slag 18

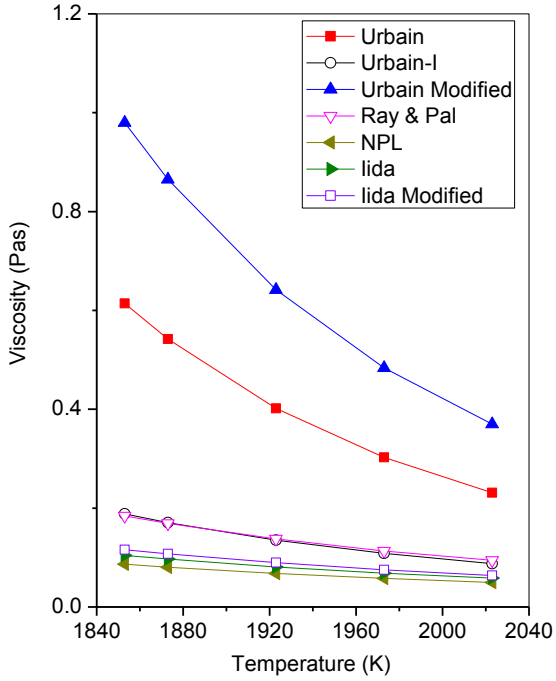

Slag 19

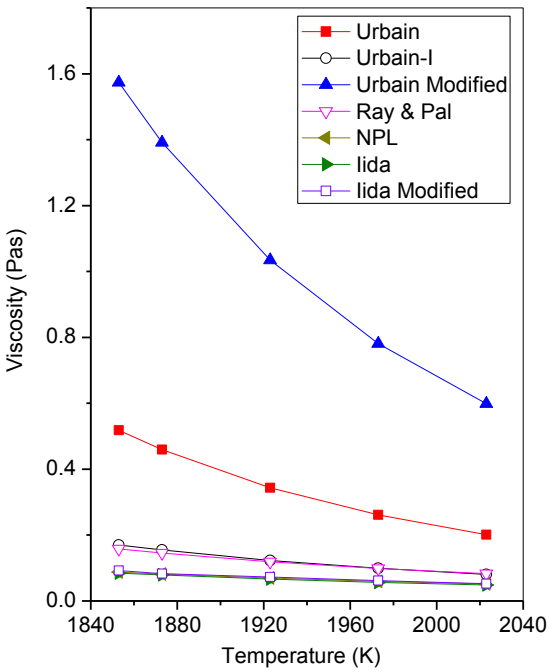

Slag 20

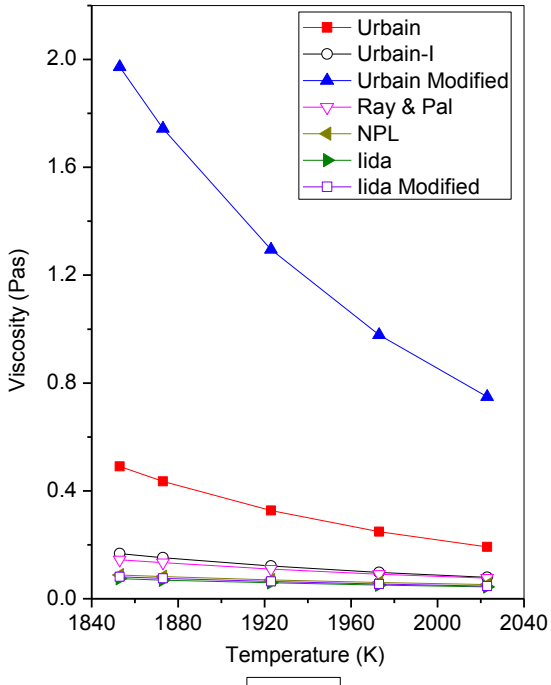

Slag 21

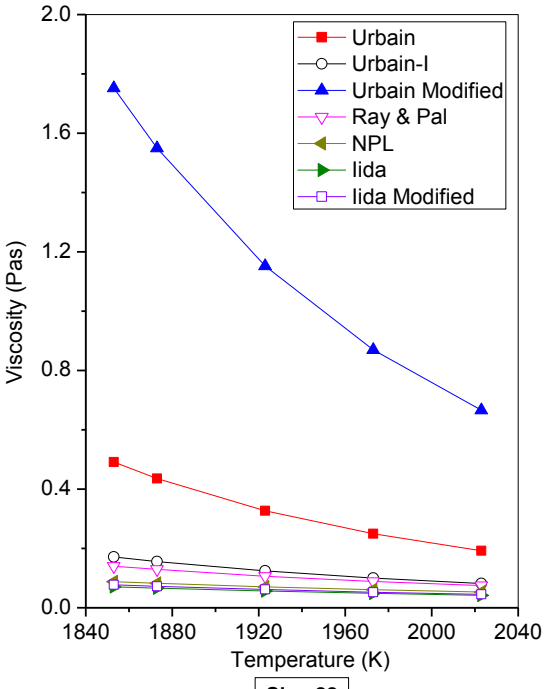

Slag 22

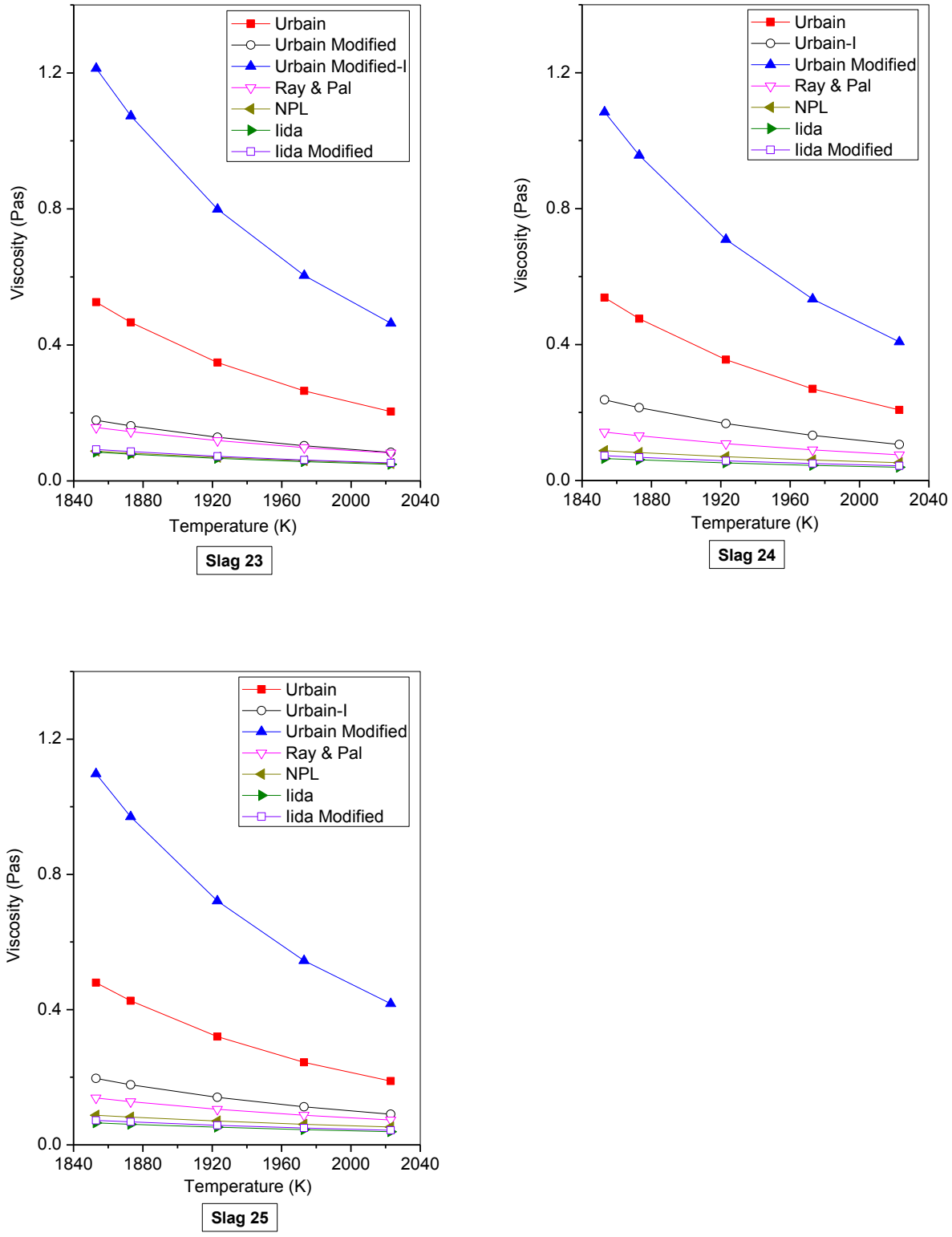

Fig.4.1. Viscosities of different slags (composition presented in Table 3.1), predicted by various viscosity models.

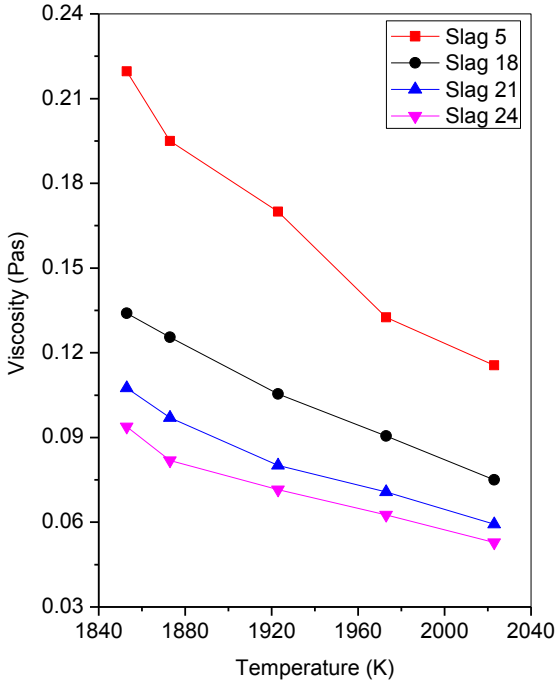

Fig.4.2. Viscosities of slags measured by the high temperature viscometer.

It is observed from the plots in Fig. 4.1, that the Urbain modified model predicts the highest viscosity values followed by the Urbain model. This prompts one to examine all the Urbain initiated models, viz. Urbain modified, Urbain and the Urbain-I model in greater details. It is observed that the Urbain modified model is based on slag systems consisting of SiO_2-Al_2O_3-CaO-FeO only, i.e., the model is generated for prediction of slag-viscosity basing principally on these oxides only. It does not consider other network modifiers such as MgO and alkali earth oxides Na_2O and K_2O. These oxides modify the silicate network forming smaller flow units and are supposed to bring down the slag viscosity. Their non-consideration, therefore, is likely to enhance the slag viscosity as observed in the present study. Further, this model uses two empirical parameters ‘m’ and ‘n’ to determine ‘A’ and ‘B’ two other constitution dependent parameters. It is obvious that such use of empirical parameters to determine the constitution-dependent parameters related to limited compositional variations like SiO_2-Al_2O_3-CaO-FeO only is likely to render erroneous results.

The Urbain model is based on a term 'B' which has components B_0, B_1, B_2 and B_3 calculated based on empirical relationships. Further, though this model considers all the minor and major components usually encountered in a slag system, it is chiefly based on a CaO-Al_2O_3-SiO_2 system. It is noteworthy that out of these three constituents SiO_2 is a strong network former; Al_2O_3 is amphoteric behaving like a network former or a network modifier, depending on the presence of other constituents and CaO is the only network modifier. To sum up, this model is based on certain empirical relationships and also reflects a greater influence of network formers like SiO_2 and amphoteric oxide like Al_2O_3, considering CaO as the only network modifier. Thus as presented in Fig. 4.1, this model has predicted a relatively high viscosity values that may not be very accurate. The Urbain-I model, however, predicts a low enough viscosity value. This may be attributed to the fact that this model provides for calculation of 'B' (a constant as presented earlier), on the basis of the principal network modifiers CaO, MgO, MnO individually, thus reflecting the effect of the sum of these modifiers, considering each one separately. It is also observed that viscosity values predicted by models based on Arrhenius equations (Iida model, NPL model) are more or less independent of temperature whereas models based on Weymann-Frenkel equations (Urbain, Ray and Pal) are significantly temperature dependent. A careful observation reveals that in the models of the later type an additional temperature term is provided, thus reflecting their temperature dependence where as in the models of the earlier type this additional term is missing.

As reported by many researchers [11-13], it is also observed that the measured viscosity values are best fitted with the viscosity values predicted by Iida model. This leads one to analyse the viscosity of BF slag obtained by Iida model. As evident from Fig. 4.1 and Table 3.1, when C/S ratio is kept constant, at a fixed MgO content of the slag the slag viscosity decreases with decrease of Al_2O_3. This is reflected in the plots for Slag 1 and Slag 4

with a C/S ratio of 1.0 approximately and MgO content of 6.5 weight percent. Further, when C/S ratio is fixed at 1.1 approximately, at fixed MgO contents of 10.09 and 10.40 respectively for slags (Slag 9 and Slag 10) & (Slag 12 and Slag 14), the slag viscosity increases with increase in Al_2O_3 content in the absence of Na_2O, K_2O and MnO in the slag. This is also evident from the plots for Slag 1 and Slag 4.

It is clear from all the 25 numbers of plots in Fig. 4.1 and Table 3.1 that irrespective of Al_2O_3 and MgO variations, within the compositional variations investigated, the slag viscosity decreases with increase of C/S ratio. As evident from the plots of Slag 10 and Slag 12, when C/S ratio is constant at 1.10 approximately and Al_2O_3 is constant at 19.0 weight percentage, and the slag doesn't contain Na_2O, K_2O and MnO, an increase in the MgO content from 10.09 weight percent to 10.40 weight percent results in a decrease in slag viscosity. A similar observation can be made when viscosity data of slags (Slag 5 and Slag 3), (Slag 15 and Slag 16) & (Slag 20 and Slag 21) are compared.

4.2. Flow Characteristics

The characteristic temperatures of different slag samples are shown in Fig. 4.3.The figure does not show any specific trend between slag composition and characteristic temperatures of the slag samples investigated in the present study. However, critical examination of the result show a valid relationship between slag composition and the characteristic temperatures of the slag samples which is in line with the literature [14]. The characteristic temperature decreases with increase in C/S ratio[14]. An increase in C/S ratio increases the CaO content which breaks the silicate network into smaller flow units [21], resulting a decrease of viscosity. Since smaller flow units require relatively higher oxygen, rendered by the addition of higher amounts of basic oxide (CaO), the progressive increase in oxide content is less, and less effective in decreasing the flow unit size [21].However, at

higher C/S ratio (> 1.1) the characteristic temperatures of the slag should decrease as the presence of stronger base increases [26]. Similarly, high MgO content decreases the characteristics temperature. However, such decrease is insignificant beyond 10% of MgO in the blast furnace slags. At higher CaO content when Al_2O_3/CaO ratio is less than 1, Al adopts 4-fold co-ordination and behaves like a network former along with SiO_4 in the melt. In case this ratio increases beyond 1 i.e. when sufficient oxygen is not available Al adopts a 6-fold co-ordination with oxygen and enters with interstices of the structure and behaves like a network breaker [26]. Hence, an increase Al_2O_3in content increases the characteristic temperatures. The minor constituent like Na_2O, K_2O, FeO, MnO and TiO_2 generally decreases the characteristic temperatures of the slag. In the present study, it may be observed that the slag samples of high C/S ratio (≥ 1.1) have higher characteristic temperatures (Slag 15 – Slag 25). The effect of MgO content on characteristic temperatures is in line with literature. For example, Slag 10 and Slag 12 have equal percentages of Al_2O_3 and approximately equal C/S ratio in addition to the minor constituents, which show a decrease in characteristics temperature with increase in MgO content of the slag. Similarly, the slag samples with lower percentages of Al_2O_3 content show relatively lower characteristic temperatures (Slag 2, Slag 8 and Slag 18). Slag 8 and Slag 13 possess approximately equal values of C/S ratio and MgO content, and these slags show an increasing trend in characteristic temperatures with increase in Al_2O_3 content.

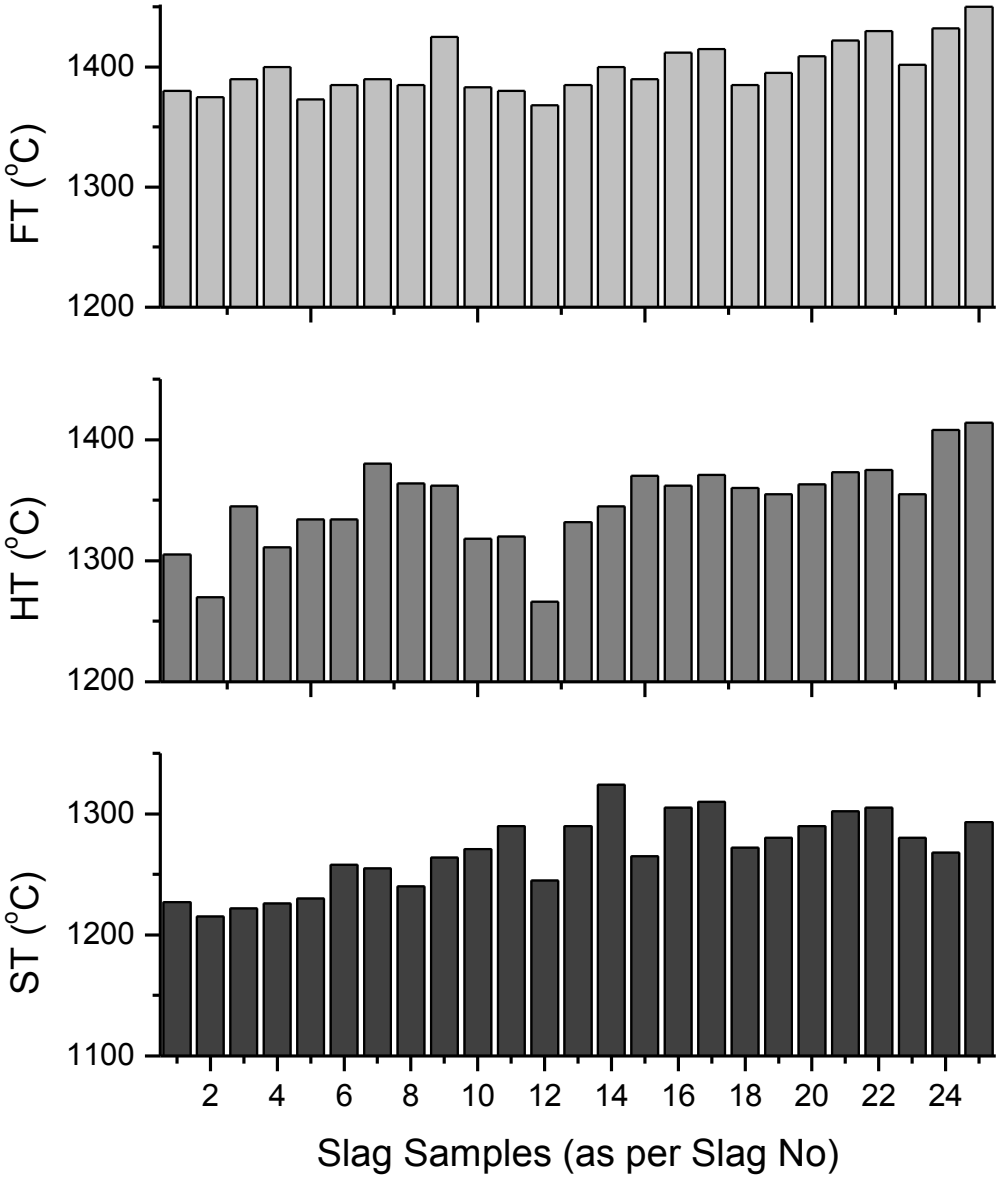

Fig. 4.3 Characteristic temperatures, obtained from heating microscope, of different slag samples.

4.3. X-ray Diffraction and Microscopic Analysis

The XRD plots of slowly cooled slag samples are shown in Fig. 4.4. It may be noted that the slags so generated are in granulated form and do not show any crystalline phases. However, after slow cooling from liquid, it shows different crystalline phases. From Fig. 4.4, the following observations can be made:

- The major phases present in the slag samples are *melilite, akermanite-gehlenite, merwinite* whereas the minor phase observed is *spinel.*
- Samples with high MgO content (≥ 10%) show spinel and merwinite phases apart from melilite phase. But with low MgO content (< 10%), the crystalline phase is melilite only.
- Samples with low C/S ratio (≤ 1.05) and low MgO content (≤ 8%) have dominant melilite phase.
- Samples with high C/S ratio (1.4) and high MgO content (11%) have merwinite phase apart from gehlenite and magnesia in the range of gehlenite-akermanite.

The phases observed in the slag samples are very much comparable with the ternary phase diagram of CaO-MgO-SiO_2 with 20% Al_2O_3 (Fig. 4.5). Slag samples with low C/S ratio of 0.94, 1.00, 1.05 & 1.09 with respective MgO content of 6.51%, 6.50%, 10.09% & 10.40% correspond to the gehlenite-akermanite region in the phase diagram. Similarly slag samples with C/S ratio of 1.23 & 1.4 with respective MgO content of 10.89% and 11.01% correspond to additional merwinite and spinel region apart from melilite region of the phase diagram. As evident from Fig. 4.6, the ternary phase diagram of CaO-MgO-SiO_2 with 15% Al_2O_3, the slag samples with low C/S ratio (< 1) and low MgO content (< 10%) correspond to anorthite region of the phase diagram and a lower melting temperature of the slag may be obtained.

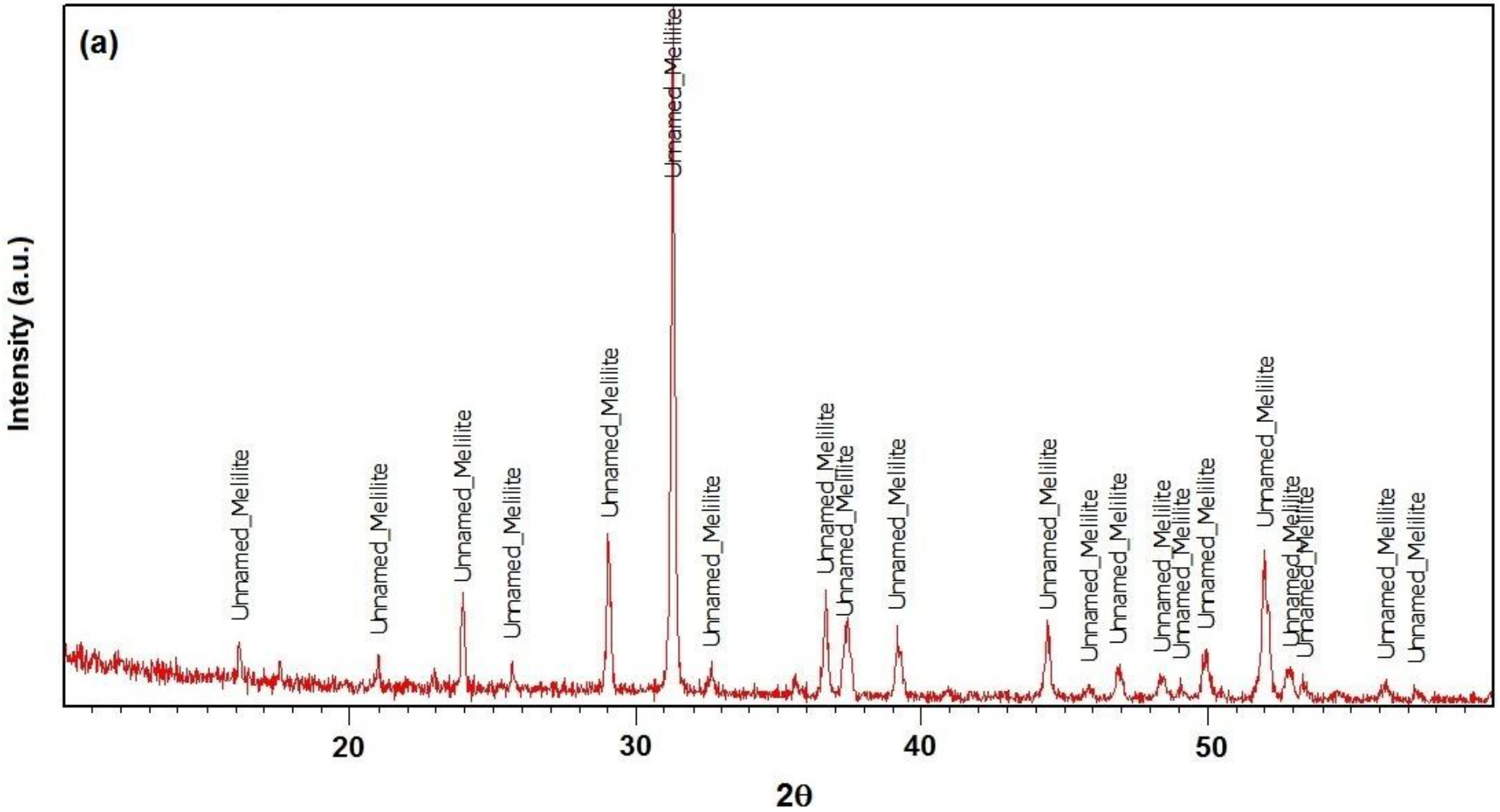
(a)
Intensity (a.u.)
Unnamed_Melilite
20
30
40
50
2θ

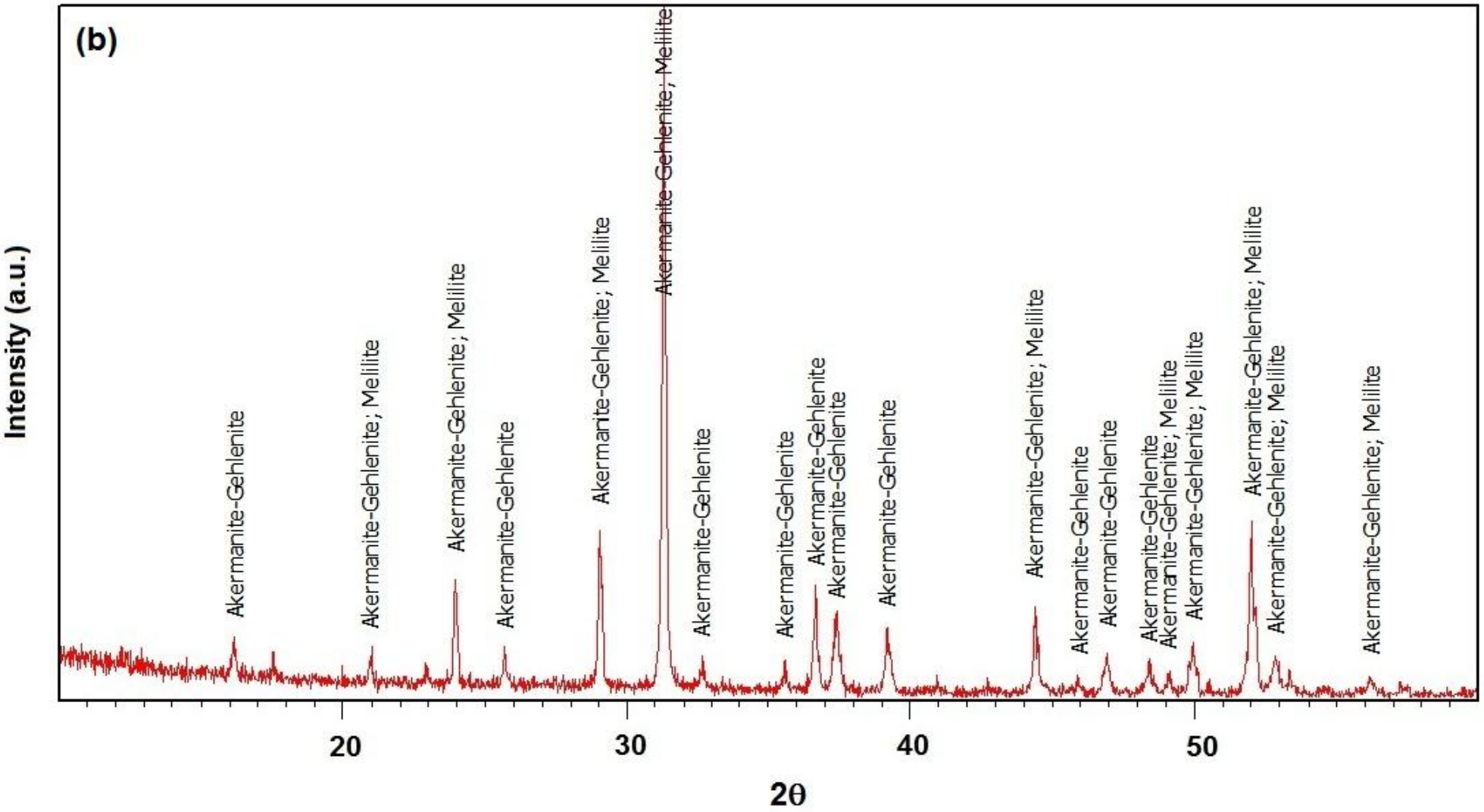
(b)
Intensity (a.u.)
Akermanite-Gehlenite
Akermanite-Gehlenite; Melilite
Akermanite-Gehlenite; Melilite
Akermanite-Gehlenite
Akermanite-Gehlenite; Melilite
Akermanite-Gehlenite; Melilite
Akermanite-Gehlenite
Akermanite-Gehlenite
Akermanite-Gehlenite
Akermanite-Gehlenite
Akermanite-Gehlenite; Melilite
Akermanite-Gehlenite
Akermanite-Gehlenite
Akermanite-Gehlenite
Akermanite-Gehlenite; Melilite
Akermanite-Gehlenite; Melilite
Akermanite-Gehlenite; Melilite
Akermanite-Gehlenite; Melilite
Akermanite-Gehlenite; Melilite
20
30
40
50
2θ

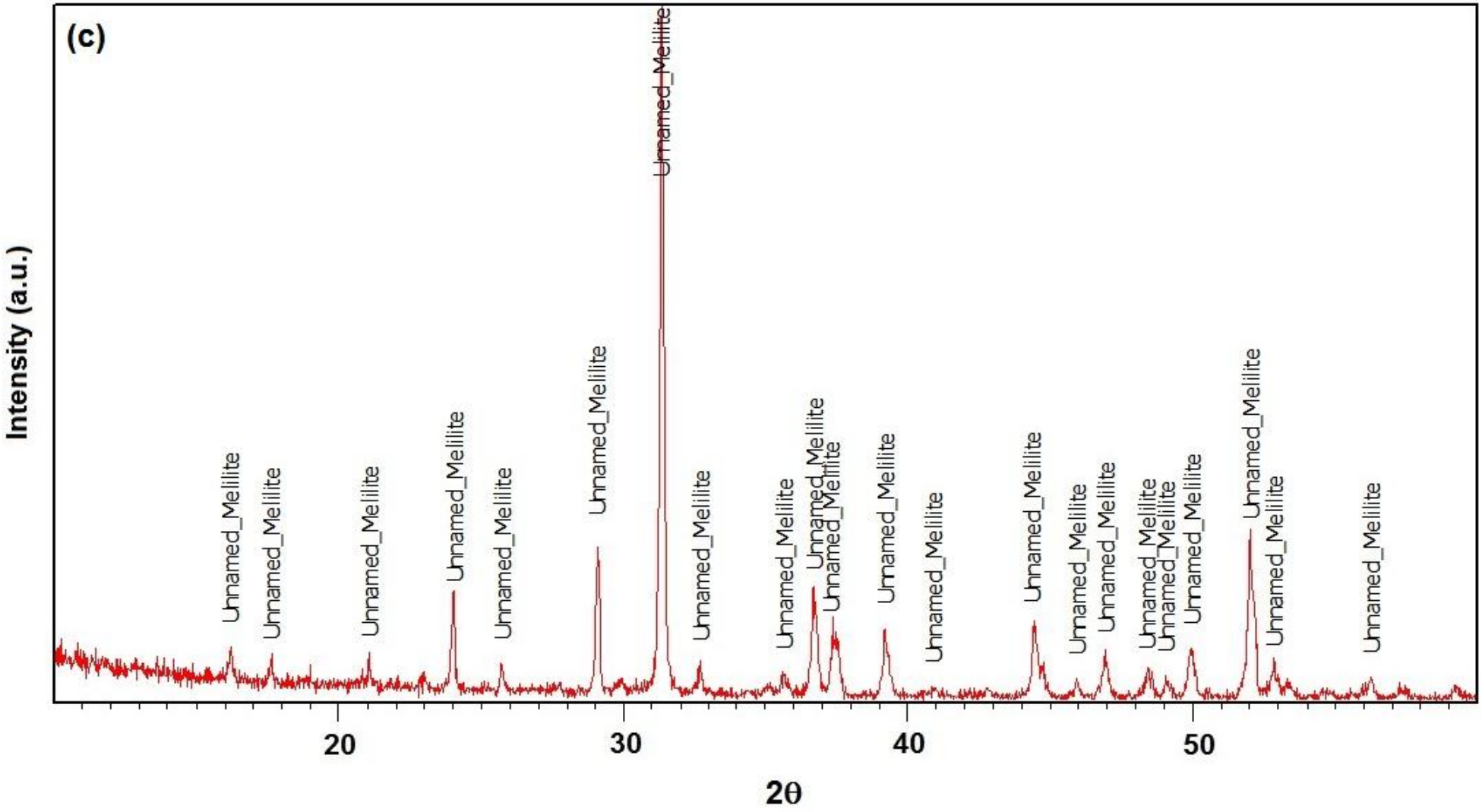
(c)
Intensity (a.u.)
Unnamed_Melilite
Unnamed_Melilite
Unnamed_Melilite
Unnamed_Melilite
Unnamed_Melilite
Unnamed_Melilite
Unnamed_Melilite
Unnamed_Melilite
Unnamed_Melilite
Unnamed_Melilite
Unnamed_Melilite
Unnamed_Melilite
Unnamed_Melilite
Unnamed_Melilite
Unnamed_Melilite
Unnamed_Melilite
Unnamed_Melilite
Unnamed_Melilite
Unnamed_Melilite
Unnamed_Melilite
Unnamed_Melilite
20
30
40
50
2θ

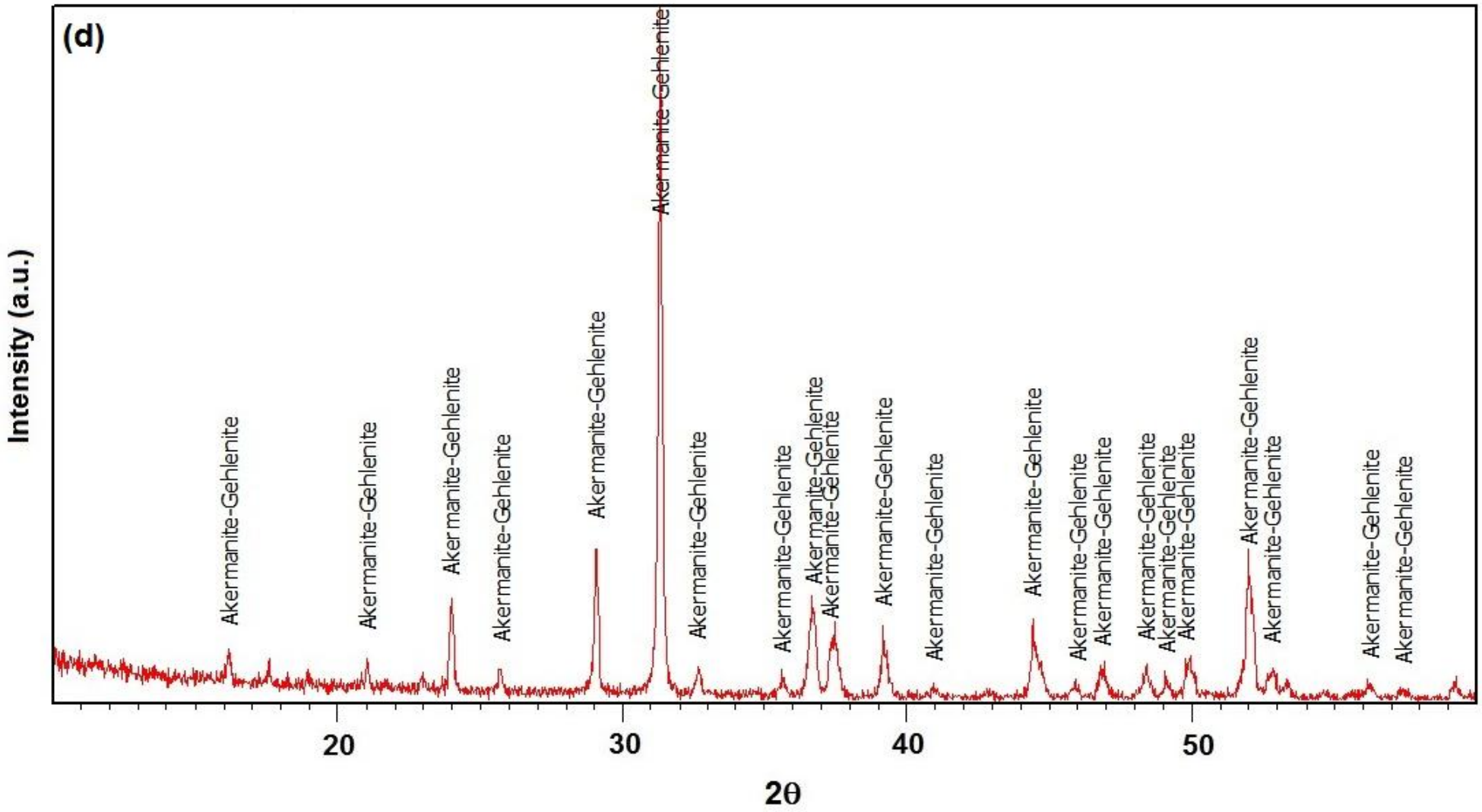
(d)
Intensity (a.u.)
Akermanite-Gehlenite
Akermanite-Gehlenite
Akermanite-Gehlenite
Akermanite-Gehlenite
Akermanite-Gehlenite
Akermanite-Gehlenite
Akermanite-Gehlenite
Akermanite-Gehlenite
Akermanite-Gehlenite
Akermanite-Gehlenite
Akermanite-Gehlenite
Akermanite-Gehlenite
Akermanite-Gehlenite
Akermanite-Gehlenite
Akermanite-Gehlenite
Akermanite-Gehlenite
Akermanite-Gehlenite
Akermanite-Gehlenite
Akermanite-Gehlenite
Akermanite-Gehlenite
20
30
40
50
2θ

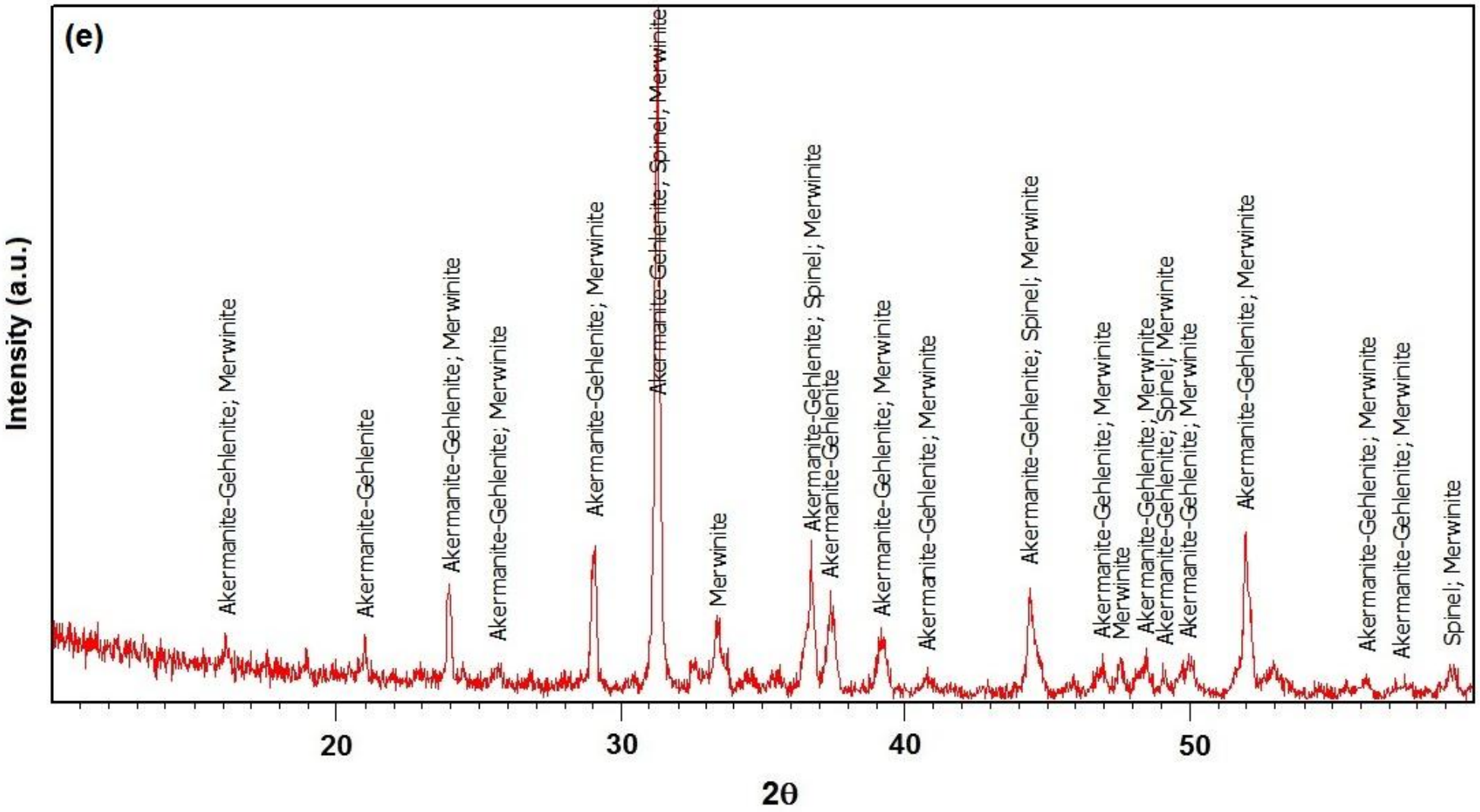
(e)
Intensity (a.u.)
Akermanite-Gehlenite; Merwinite
Akermanite-Gehlenite
Akermanite-Gehlenite; Merwinite
Akermanite-Gehlenite; Merwinite
Akermanite-Gehlenite; Merwinite
Akermanite-Gehlenite; Spinel; Merwinite
Merwinite
Akermanite-Gehlenite; Spinel; Merwinite
Akermanite-Gehlenite
Akermanite-Gehlenite; Merwinite
Akermanite-Gehlenite; Merwinite
Akermanite-Gehlenite; Spinel; Merwinite
Akermanite-Gehlenite; Merwinite
Merwinite
Akermanite-Gehlenite; Merwinite
Akermanite-Gehlenite; Spinel; Merwinite
Akermanite-Gehlenite; Merwinite
Akermanite-Gehlenite; Merwinite
Akermanite-Gehlenite; Merwinite
Akermanite-Gehlenite; Merwinite
Spinel; Merwinite
20
30
40
50
2θ

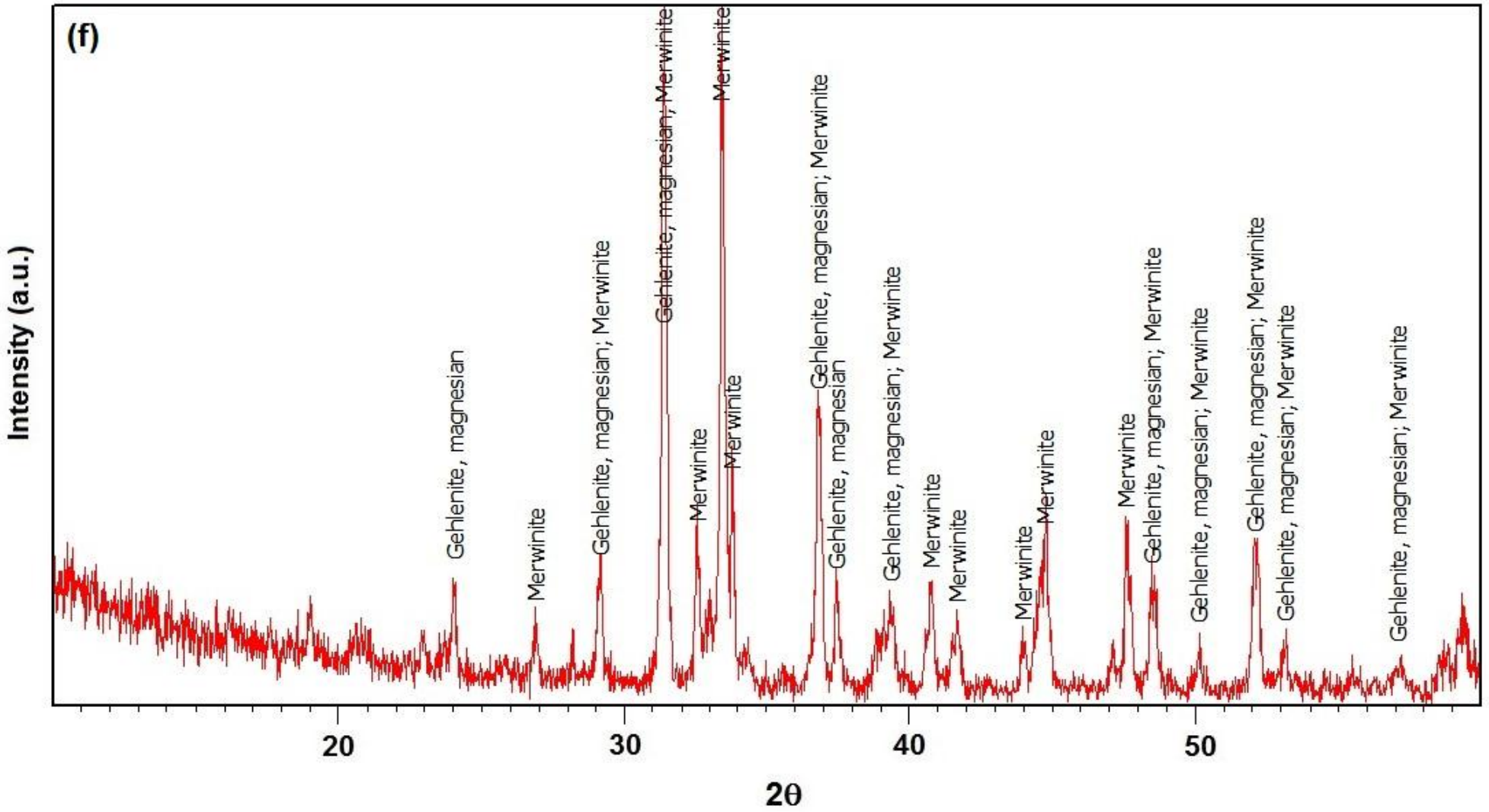

Fig. 4.4. XRD plots of some selected slag samples: (a) Slag 1, (b) Slag 4, (c) Slag 9, (d) Slag 14, (e) Slag 22 and (f) Slag 24.

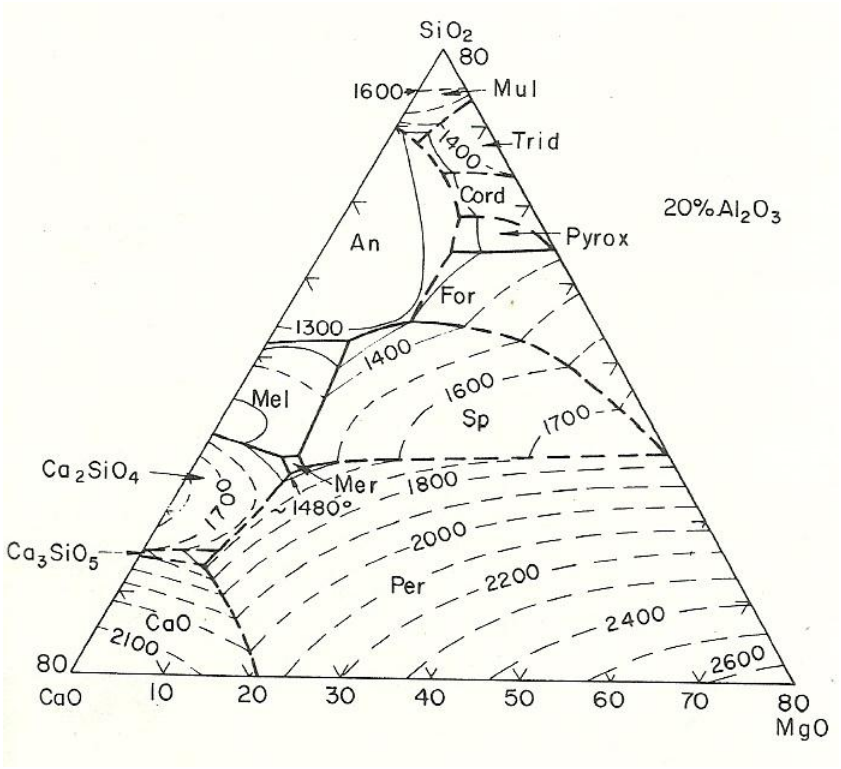

Fig. 4.5. System $CaO–Al_2O_3–SiO_2–MgO$, for 20% Al_2O_3 plane [16].

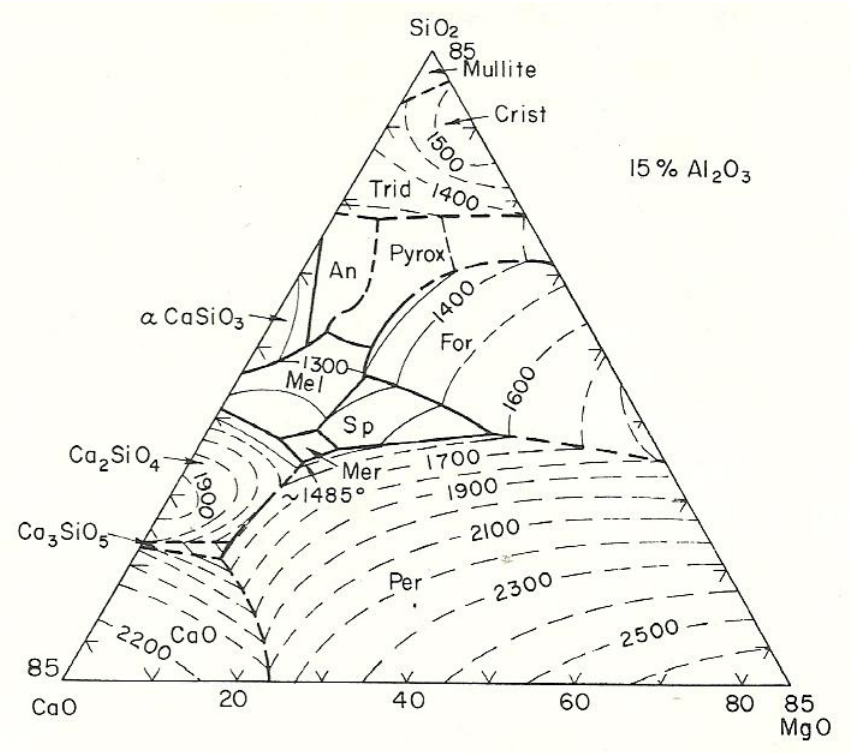

Fig. 4.6. System $CaO–Al_2O_3–SiO_2–MgO$, for 15% Al_2O_3 plane [16].

Fig. 4.7 shows the optical microstructures of the slag samples of different compositions. The figure reveals the microstructural features of different phases in the blast furnace slag samples. Major phases observed under the microscope are also observed in XRD analysis. The phases like calcium ferrite (in Slag 12) or di-calcium aluminate (Slag 19) are also observed because of higher amount of iron oxide content and high Al_2O_3&CaO content in the slags respectively.

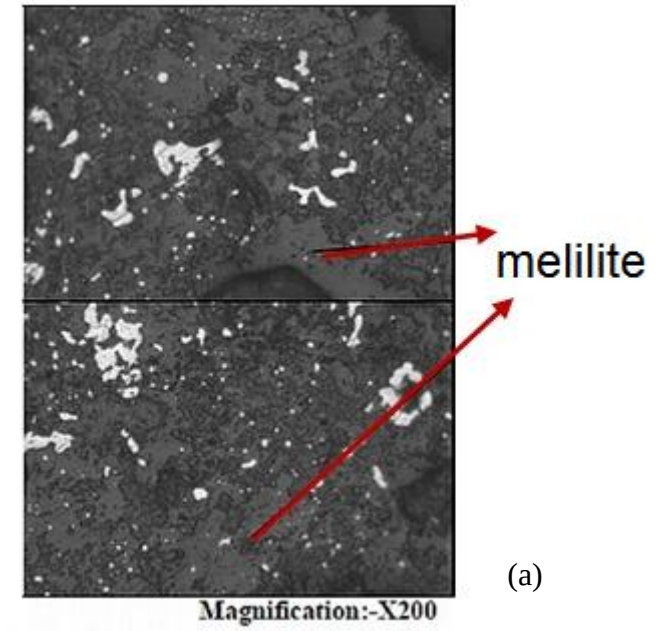

(a)

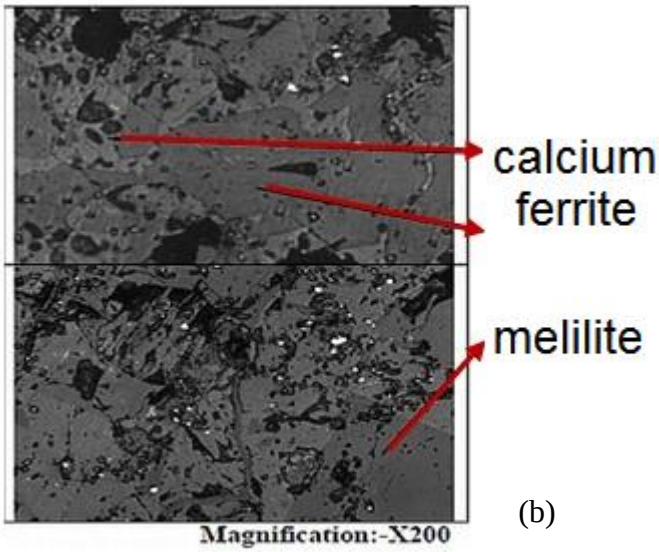

(b)

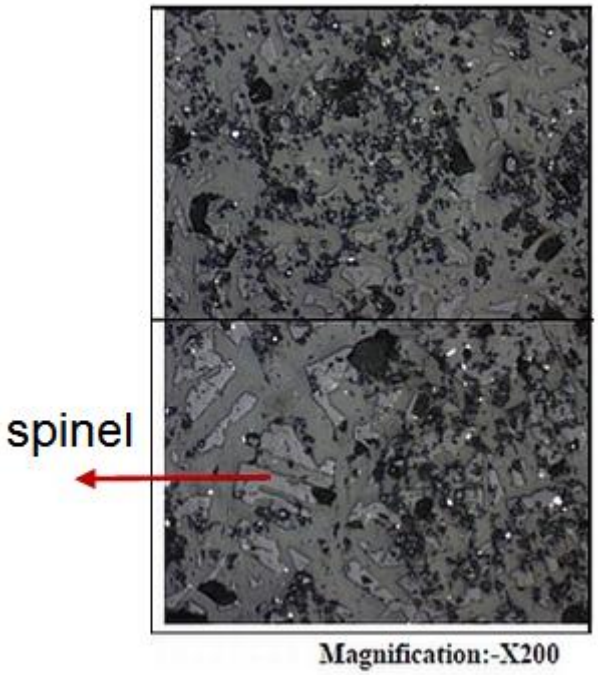

(c)

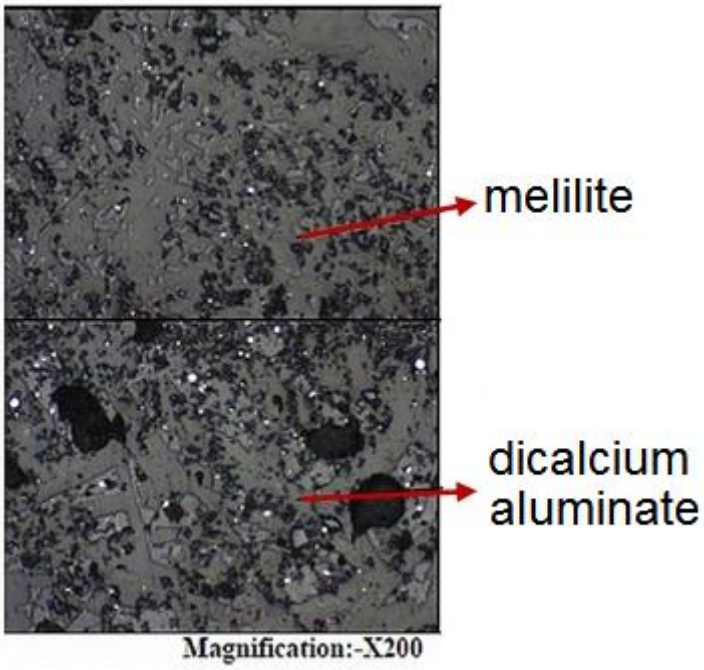

(d)

Fig. 4.7. Optical microstructures of some selected slag samples: (a) Slag 4, (b) Slag 12, (c) Slag 17 and (d) Slag 19.

5. Summary

From the present investigations, the following conclusions can be made:

(i) Urbain modified model predicts a high viscosity value probably because it doesn't consider all the network modifiers. Urbain model is proposed basing on certain empirical relations and may not predict accurate viscosity data for the blast furnace slag. Urbain I model considers the network modifiers CaO, MgO and MnO individually and renders a low enough viscosity value. For models based on Arrhenius type of equations the predicted viscosity values are more or less independent of temperature variations.

(ii) Blast furnace slag viscosity decreases with increase of C/S ratio when varied between approximate values of 1.0 to a value of 1.4. At a constant C/S ratio and MgO contents slag viscosity increases with increase in Al_2O_3 content. The vice versa is also true. At a constant C/S ratio and constant Al_2O_3 content the blast furnace slag viscosity decreases with increase of MgO content.

(iii) The slag samples of high C/S ratio ($\geq$ 1.1) have higher characteristic temperatures. A decrease in characteristics temperatures with increase in MgO content of the slag is observed. Similarly, the slag samples with lower percentages of Al_2O_3 content show relatively lower characteristic temperatures and vice-versa.

(iv) The XRD analysis reveals that the major phases present in the slag samples are melilite, akermanite-gehlenite, merwinite whereas the minor phase observed is spinel. Samples with low C/S ratio ($\leq$ 1.05) and low MgO content ($\leq$ 8%) have dominant melilite phase. Samples with high C/S ratio (1.4) and high MgO content (11%) have merwinite phase apart from gehlenite and magnesia in the range of gehlenite-akermanite.

References

1. Tiwary J N, Mishra B, Sarkar S and Mohanty U K, Emerging materials research, **2,** (2013), 152.
2. Gupta S S and Chatterjee A, Blast Furnace Iron Making, SBA Publication, Washington (1995), 20.
3. Behera R C, Mohanty U K and Mohanty A K, High Temperature Materials and Processes**, 9,** (1990), 57.
4. Kondratiev A, Jak E and Hayes P C, JOM, **54,** (2002), 41.
5. Shankar A, Gornerup M, Lahiri A K and Seetharaman S, Metallurgical and Materials Transactions B, **38,** (2007), 911.
6. Mills K C, Slag Atlas 2nd edition, Düsseldorf, Germany, **2,** (1995), 349.
7. Sridhar S, JOM, **54,** (2002), 30.
8. Mills K C, Short course presented as part of Southern African Pyro-metallurgy 2011, **1,** (2011), 56.
9. Ray H S and Pal S, Ironmaking and Steelmaking, **31,** (2004), 125.
10. Mills K C and Sridhar S, Ironmaking and Steelmaking, **26,** (1999), 262.
11. Iida T, Sakai H, Kita Y and Shigeno K, ISIJ International, **40,** (2000), S110.
12. Iida T, 5th Int. Conf. Molten Slags, Fluxes and Salts, Warrendale, PA: ISS, (1997), 877.
13. Iida T, Proceedings of the Mills Symposium, London, (2002), 101.
14. Dash S, Mohanty N, Mohanty U K, Sarkar S, Open journal of Metal, **2,** (2012), 242.
15. Gupta V K and Sheshadri V, Trans.IIM, **26,** (1993), 55.
16. Singh R N, Steel India, **7,** (1984), 73.
17. Kondratiev A and Jak E, Metallurgical and Materials Transactions B, **32,** (2001), 1015.
18. Kekkonen M, Oghbasilasie H and Louhenkilpi S, Department of materials science and engineering, research report, science and technology, Aalto university publication

series,**12** (2012), 6.

19. Bird R B, Stewart W E and Lightfoot E N, Transport Phenomena, New York: John Wiley & Sons, **2,** (2002), 20.
20. Sridhar S, Steel Research, **70,** (2001), 3.
21. Mills K C, Viscosities of Molten Slags, Teddington, U.K.: NPL, (1992), 46.
22. Iida T, Morita Z and Mizobuchi T, Proc. of the 3rd International Conference on Molten slags and fluxes, London Institute Of Materials, (1988), 888.
23. Kim J W, Proc 4th Intl. Conf, Molten Slags and Fluxes, Tokyo: ISIJ, (1992), 468.
24. Seetharaman S, Sichen Du, Ji F.Z, Met Mat.Trans. B, **31**, (1999), 105.
25. Gupta D, Sridhar S, ALCOA-DOE Report, (2001).
26. Mohanty U K, "Thermo Physical Properties of Some Metallorthermic Slags," Ph.D. Dissertation, R.E. College, Rourkela, (1998), 54.
27. Stephan K, Lucas K, Viscosity of Dense Fluids, Plenum, New York, **2**(1979), 461.
28. Watt J D and Fereday F, The flow Properties of the slags formed from the ashes of British coals. Part I. Viscosity of Homogeneous Liquid Slags in Relation to Slag Composition, J. Inst. Fuel, **42,** (1969), 101.
29. Mills K C, Viscosities of Molten Slags, Slag Atlas, VerlagSthleisen GmbH, Dusseldorf, **2**, 1995, 349.
30. Richardson F D, Physical Chemistry of Melts in Metallurgy, New York: Academic Press, **1,**(1974), 81.
31. Sahoo S K, Tiwari J N, Mohanty U K**,** Metallurgical and Material Transaction B Issue 6, **44,** (2013), 1371.
32. Urbain G, Viscosity estimation of Slags, Steel Res., **58,** (1987), 111.
33. Seetharaman S and Sichen D, ISIJ Int., **37,** (1997), 109
34. Hopkins D W, Davenport W G, Peacy J G, Technology and engineering theory and

practice, (2013), 38.

35. Mills K C and Keene B J, Intern. Mat. Rev., **32** (1987), 120.
36. Park J H, Min D J and Song H S, ISIJ Int., **42** (2002), 344.
37. Mishra U N, Thakur B and Thakur M.N, SEAISI Q., **23** (1994), 72.
38. Fredericci C, Zanotto E D and Ziemath E C, Crystallization mechanism and properties of a blast furnace slag glass. J. Non-Cryst.Solids, **64,** (2000), 273.
39. Kaiura G H, Toruri J M and Marchant G, Can. Metall. Q., **16,** (1977), 156.
40. Urbain G, Bottinga Y and Richet P, GeochimCosmochim, Acta, **46,** (1982), 1061.
41. Solomin I., Conf. on Visc.Liquids and Coll.Solutions, **1,** (1941), 317.
42. Paul M., Principles of Chem.Thermodynamics, New York, (1951), 146.
43. Bockris J O'M. and Lowe D C, Royal Soc., **226,** (1954), 423.
44. Bockris J O'M, Kitchener J A and Machenzie J D, Trans Faraday Society, **51,** (1955), and 1735.
45. Endell K and Hellbriigee J, Naturwissenschaften, **30**, (1942), 421.
46. Bockris J O'M, Tomlinson J W and White J L, Trans.Faraday Soc.,**52** (1956), 299.
47. Toop G W, M.A.Sc Thesis, University of British Colombia, **4**, (1960).
48. Toop G W and Semis C S, Trans. Met. Soc. AIME, **224**, (1962), 878.
49. Toop G W and Semis C S, Can.Met.Quarterly, **1**, (1962), 129.
50. Fincham C J B, and Richardson F D, Proc.Roy.Soc.**40 (A)**, (1954), 223.
51. Temkin M, ActaPhysiochim. **20**, (1945), 411.
52. Masson C R, Proc.Royal.Soc. (London), **287**, (1965), 201.
53. Masson C R J. Am.Ceram.Soc., **51**, (1968), 134.
54. Whiteway S G, Smith I B, and Masson C R, Can. J. Chem, **48**, (1970), 33.
55. Masson C R, Smith I.B, Whiteway S G, IBID, P, (1456).
56. Gaskel D R, Can. Metallurgical Quarterly, **20**, (1981), 19.

57. Volarovitch M, and Leontievan A, J.Soc.Glass Tech, **20**, (1936), 139.

58. Lacy E D, J. of Physical Chem. Of Glasses, **6**, (1965), 171.

59. Mysen B O, Earth Science Rev., **27**, (1990), 281.

60. Mackenzie J D, Trans.FaradaySos, **53**, (1957), 1488.

61. Weyl W A, J.Soc, Glass Tech, **35**, (1951), 421.

62. Kozakevitch P, International Symposium on Phy.Chem of Process Metallurgy, AIME, **7**, (1959), 116.

63. Machin J S and Hanna D L, J.Am.Cer.Soc.**28**, (1945), 310.

64. Moore H and McMillan P W, J.Soc.Glass.Tech. **40**, (1956), 193.

65. Seshadri V and Gupta V K, Arch., Eiseniittenwes, **45**, (1974), 337.

66. Gupta V K and Seshdri V, Silver Jubilee Symposium, Process metallurgy, Ind.Inst.Met, (1972), 203.

67. Turkdogan E T and Bills P M, Am.Cer.Bull, **39**, (1960), 682.

68. Kuchariski M, Stubina N M, and Toguri J M, Can.Met.Quarterly, **28 (1)**, (1989), 11.

69. Waseda Y, Shiraishi Y and Toguri J M, Trans. Japan.Inst.Metals, **21** (1980), 51.

70. Moringa K, Suginohara Y, Yanagase T, J. Japan. Inst.Met, **40**, (1976), 480 and 775.

71. Bills P M, JISI, **20**, (1963) 133.

72. Nesteronko S V and Khomenko V M, Russ.Met, **5**, (1982), 35.

73. Yanganese T and Nakamura T, J.Jap.Inst.Met, **41,** (1977), 165.

74. Mills K C, ISII International, **33**, (1933), 148.

75. Duffy J A, Iron and Steel Making, **17**, (1990), 410.

76. Machine J S and Yee T B, J.Am.Cer.Soc, **31**, (1948), 200.

77. Machine J S, Yee T B and Hanna D L, J.Am. Cer.Soc, **35**, (1952), 322.

78. Mahine J S and Yee J B, J.Am.Cer.Soc.**37**, (1954), 177.

79. Yakusev, Romashin V M and Amfiteatrov V A, Steel in USSR, **7**, (1977), 617.

80. Kawahara M, Moringaga K J, and Yanagase T, Can.Mett.Quarterly, **22,** (1983), 143.

81. Golatonov A.L, STAL in English, **6**, (1964), 425.

82. Sokolov G A, and Gul'tyai I I, STAL in English, **12**, (1965), 951.

83. Yakubtsiner N M, Machinkii V G and Panyshin L A, STAL in English, **3**, (1968), 184.

84. Singh N, Muthykrishnan V and Rajozinski T, MML Tech. Journal, **12**, (1970), 12.

85. Gupta V K, and Seshadri V, Trans.Ind.Inst.Met, **26**, (1973), 55.

86. Richardson F D, Physical Chemistry of Melts in Metallurgy, Volume 1 and New York: Academic Press, (1974), 81.

87. Urbain G, Bottinga Y and Richet P, GeochimCosmochim, Acta, **46,** (1982), 1061.

88. Urbain G, Steel Research, **58,** (1987), 111.

89. Shankar A, "Studies on high alumina blast furnace slags", Doctoral thesis, School of Industrial Engineering and Management, Royal Institute of Technology, SE 10044, Stockholm, KTH (2007).

90. Duffy J A and Ingram M D, J. Amer. Chem. Soc., **93,** (1971), 6448.

List of Publications

1. Pati A, Mishra B, Mohanty U K and Sahoo S K, *Estimation of viscosity of Industrial Blast Furnace Slag in Indian Scenario and its Analysis*, ISRS 2014, IIT Madras, December 11-13, (2014).
2. Pati A, Sahoo S K, Mishra B and Mohanty U K, *Viscosity of Industrial Blast Furnace Slag in Indian Scenario,* Communicated to Transactions of IIM, June, (2015).